Mediterranean Geoscience Reviews (2019) 1:55–90
https://doi.org/10.1007/s42990-019-00004-6

ORIGINAL PAPER

Integrated biostratigraphy of the middle to upper Eocene Kırkgeçit Formation (Baskil section, Elazığ, eastern Turkey): larger benthic foraminiferal perspective

Ercan Özcan[1] · Gy. Less[2] · L. Jovane[3] · R. Catanzariti[4] · F. Frontalini[5] · R. Coccioni[5] · M. Giorgioni[3,6] · D. Rodelli[3] · E. S. Rego[3,7] · S. Kayğılı[8] · M. Asgharian Rostami[9]

Received: 9 April 2019 / Revised: 16 June 2019 / Accepted: 22 June 2019 / Published online: 10 July 2019

Abstract
The Baskil section, located to the west of Elazığ in eastern Turkey, represents deep-marine facies of the Eocene Kırkgeçit Formation, deposited in a wide spectrum of environmental conditions ranging from shelf to basin. The 390-m-thick sequence was deposited at bathyal depths in the Tethys, at the edge of the subsiding Anatolide–Tauride plate and is highly promising for an integrated study of Bartonian to earliest Priabonian mid-latitude neritic and deep-marine biota. The section contains numerous allochthonous limestone beds, characterized either by turbidites or debris flows with resedimented larger benthic foraminifera (LBF). The section spans the planktonic foraminiferal Zones E10/11 to E14, the calcareous nannofossil zones NP15–NP18, shallow benthic zones (SBZ) SBZ16/17 to SBZ18A, including orthophragminid (OZ) zones OZ12–OZ14. The Bartonian–Priabonian boundary is placed at NP17/18 boundary by the lowest occurrence of *Chiasmolithus oamaruensis,* which lies within Subchron C17n.1n and Zone SBZ18A. The LBF, obtained as loose specimens from 17 turbiditic and debris flow beds, are characterized predominantly by 21 orthophragminid lineages and 13 nummulitid species as well as some other stratigraphically diagnostic genera. Most of the orthophragminid lineages straddle the Bartonian–Priabonian boundary, whereas *Orbitoclypeus douvillei* and *Discocyclina pulcra* appear to be the only orthophragminids confined to SBZ17 at its upper range. The *Nummulites fabianii*-lineage first appearing in zones E12 and NP16 in the Bartonian shows a well-documented evolution of the embryon, and is referred to *Nummulites garganicus* in the Bartonian, whereas its successor *Nummulites hormoensis* straddles the Bartonian/Priabonian boundary. The first appearances of *N. hormoensis* and *Heterostegina armenica* as well as the last occurrences of *Nummulites ptukhiani* and *Assilina exponens* in the section are almost coeval and are utilized to mark SBZ17–18 boundary. The first appearance of the *H. armenica*-lineage is recorded in zones E14 and upper part of NP17. Two important species, *Chapmanina gassinensis* and *Silvestriella tetraedra*, have been first recorded in SBZ18A just above the Bartonian–Priabonian boundary. Thus, the transition of *N. garganicus* to *N. hormoensis*, the first appearances of *H. armenica*, *C. gassinensis* and *S. tetraedra* as well as the last occurrences of *N. ptukhiani*, *Assilina exponens*, *Discocyclina pulcra* and *Orbitoclypeus douvillei*, all across the SBZ17–18 boundary or within the SBZ18A, appear to be the most useful bioevents in the transition from the Bartonian to the Priabonian in shallow-marine realms.

Keywords Bartonian–Priabonian · E Turkey · Larger benthic foraminifera · Calcareous nannoplankton · Planktic foraminifera · Magnetostratigraphy

Introduction

The integration of shallow-marine and deep-marine biota is essential for high-resolution stratigraphic applications and correlations. It requires the study of suitable stratigraphic sections yielding fossil groups representing both neritic and deep-marine realms. During the Eocene, the integration of these fossil groups in the Bartonian–Priabonian interval has been notably hampered either by the rarity of

This paper is dedicated to the late Prof. Josep Serra-Kiel from Barcelona for his outstanding contribution to Paleogene LBF.

✉ Ercan Özcan
ozcanerc@itu.edu.tr; ercanozcan034@yahoo.com

Extended author information available on the last page of the article

such stratigraphic sections or the poor occurrence of larger benthic foraminifera (hereafter LBF) in deep-marine settings, such as in the Urtsadzor section (Armenia) (Cotton et al. 2017) and the Alano di Piave section (Italy), which is candidate for the global boundary stratotype section and point (GSSP) for the Priabonian stage (Agnini et al. 2011). The Alano di Piave section yielded only two horizons with limited LBF fauna, not yet described at species level, and the Urtsadzor section consists of seven levels with only Priabonian LBF. The Miralles–La Tossa composite section from the Eastern Ebro Basin (Spain) plays a significant role in the re-evaluation of the SBZ18 Zone with respect to the Bartonian–Priabonian boundary in shallow-marine environments (Costa et al. 2013). According to Costa et al. (2013), the Zone SBZ18, the lower boundary of which is traditionally accepted to mark the Bartonian–Priabonian boundary in the Tethys (Serra-Kiel et al. 1998), extends to the early Priabonian. This notion was recently followed in the updated scheme of Tethyan Eocene SBZ zones by Papazzoni et al. (2017). Some efforts to correlate the shallow benthic and calcareous plankton zones at the Bartonian–Priabonian boundary were also made at the Varignano section in northern Italy, consisting of several bioclastic levels with resedimented LBF (Luciani et al. 2016). In this section, an integrated correlation scheme was not presented, though the potential of the section for recording the LBF events was emphasized.

The Kırkgeçit Formation crops out in a wide area from Malatya to Lake Van in eastern Turkey, to the north of Bitlis–Zagros suture zone, a major tectonic element separating the Arabian and Anatolide–Tauride plates (Fig. 1). The unit consists of a wide range of lithofacies associations, and fossil assemblages indicating various depositional environments, from very shallow-marine to pelagic, and ages ranging from the middle Eocene to the Oligocene, showing the diachronic development of the unit in eastern Turkey (Türkmen et al. 2001; Herece and Acar 2016). In the Baskil region, the middle to upper Eocene Kırkgeçit Formation is about 2259 m thick (Özkul 1988). It consists of thick coarse clastic beds of inner-fan setting, followed by bathyal marls intercalated with calcarenites, turbidites, and debris flows with abundant LBF and massive shallow-marine limestone in the upper part (Fig. 2) (Özkul 1988; Özcan et al. 2006). The Baskil section corresponds only to a part of the Kırkgeçit Formation, encompassing the upper Lutetian–lower Priabonian interval.

Here, we present an integrated biostratigraphic scheme of calcareous nannoplankton, planktonic and benthic foraminifera, and LBF from the Baskil section, which corresponds to a mid-latitude paleo-setting in the Tethys. We emphasize the distribution and zonal significance of LBF, described from 17 levels in Bartonian-earliest Priabonian interval based solely on descriptions from the loose specimens. This study follows the works of Rodelli et al. (2018) and Rego et al. (2018) from the same section, having presented a magnetobiostratigarphic framework and environmental conditions, and Özcan et al. (2006), having presented the most comprehensive LBF data from the Kırkgeçit Formation in the same area with the Baskil section.

The Bartonian–Priabonian LBF record in the Tethys: a synthesis

The middle–upper Eocene shallow-marine deposits in the Tethys contain LBF mainly represented by nummulitids, orthophragminids, alveolinids and rotaliids (Schaub 1981; Racey 1995; Serra-Kiel et al. 1998, 2003, 2016; Özcan et al. 2010; Less and Özcan 2012; Hottinger 2014; Ali et al. 2018 and references therein). The dominant middle Eocene foraminiferal taxa belong to large (giant) *Nummulites*, various species of *Assilina, Operculina,* alveolinids and orthophragminids. The first appearance of *Heterostegina*, *Spiroclypeus*, *Nummulites fabianii* group, *Pellatispira*, *Chapmanina*, and *Silvestriella*, and disappearance of alveolinids and large *Nummulites* in the Bartonian and across the Bartonian/Priabonian boundary correspond to significant foraminiferal events in the Western Tethys (Serra-Kiel et al. 1998; Less and Özcan 2012). The superposition and the chronology of these events were used to better constrain the age of shallow-marine units in the Tethys. Recently detailed studies on several groups also enabled us to subdivide the shallow benthic zones SBZ18 and 19 into subzones in the late Bartonian–Priabonian interval (Fig. 3) (Less and Özcan 2012). The *Operculina gomezi*-group appears to be the most important LBF in the tentative delineation of Lutetian/Bartonian boundary since key foraminiferal events for this boundary have not been well defined yet. The *Assilina schwageri–alpina* group also occurs abundantly in Bartonian–Priabonian Tethyan deposits, although the distinction between the two species, *A. schwageri* and *A. alpina*, presents difficulties due to the lack of morphometric data. The first appearance of *Heterostegina* is perhaps one of the most significant bioevents across the Bartonian/Priabonian boundary. The *Heterostegina armenica* and *H. reticulata* lineages display a very rapid evolution and, hence, are used as a valuable proxy to date LBF events and for biostratigraphic correlations (Less et al. 2008). The most important evolutionary trend in these lineages is the reduction in the number of operculinid chambers with time, which is used in the morphometric definition of their subspecies. Similarly, the *N. fabianii*-lineage displays a significant evolution, as reflected in the increase of the proloculus size, which helps the morphometric discrimination of the successive species (Özcan et al. 2009, 2010). The genus *Spiroclypeus*, a key Priabonian taxon, also displays the reduction in the operculinid chambers and is subdivided into different species

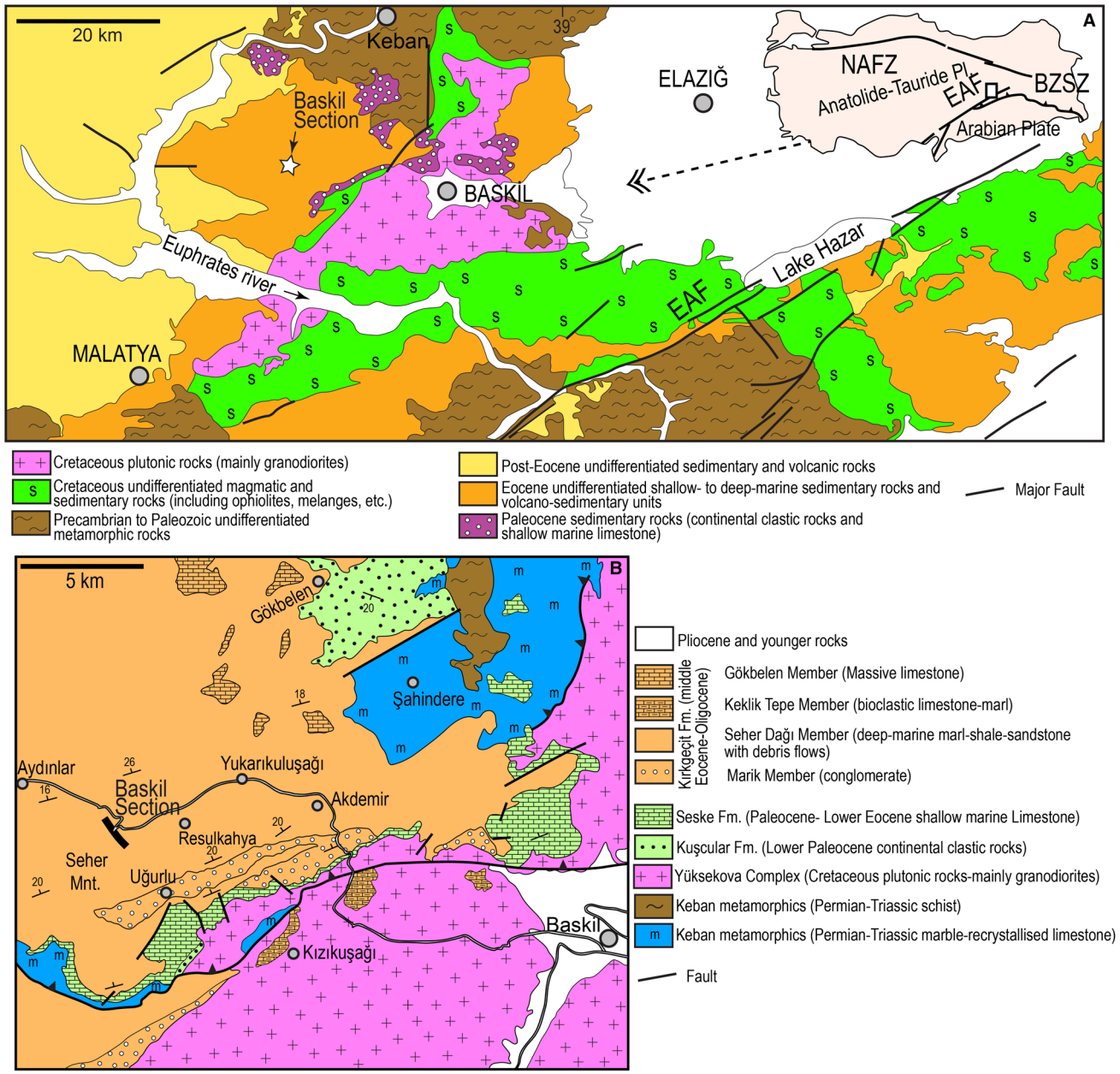

Fig. 1 **a** Geological map of the area between Malatya and Elazığ in eastern Turkey and location of the Elazığ Basin in the plate tectonics context of the region (simplified from Akbaş et al. 2011). **b** Geological map of the Baskil region with the location of the Baskil section (Özkul 1988). *EAF* East Anatolian Fault, *NAFZ* North Anatolian Fault Zone, *BZSZ* Bitlis–Zagros Suture Zone

morphometrically (Less et al. 2008). The first appearance of *Silvestriella*, *Pellatispira* and *Chapmanina* close to the Bartonian–Priabonian boundary represents a significant foraminiferal event and is very useful in the delineation of the middle/late Eocene boundary in the Tethys (Özcan et al. 2010; Luciani et al. 2016). Orthophragminids include various species of *Discocyclina*, *Nemkovella*, *Orbitoclypeus* and *Asterocyclina* (Less 1987; Özcan et al. 2006; Less et al. 2011). The extinction of taxa such as *Discocyclina pulcra* and *Orbitoclypeus douvillei* in the Bartonian, *Discocyclina pratti*, *D. discus*, *Nemkovella strophiolata*, *Asterocyclina kecskemetii*, and *A. alticostata* in the Priabonian before the onset of Priabonian/Rupelian boundary are key events. The Bartonian/Priabonian boundary, coincident with the SBZ18/19 boundary in Serra-Kiel et al. (1998), was lately lowered as to lie within the SBZ18 by Costa et al. (2013) and Papazzoni et al. (2017). In this study, we follow Less and Özcan (2012) in the assignment of subzones of SBZ18 to the studied section.

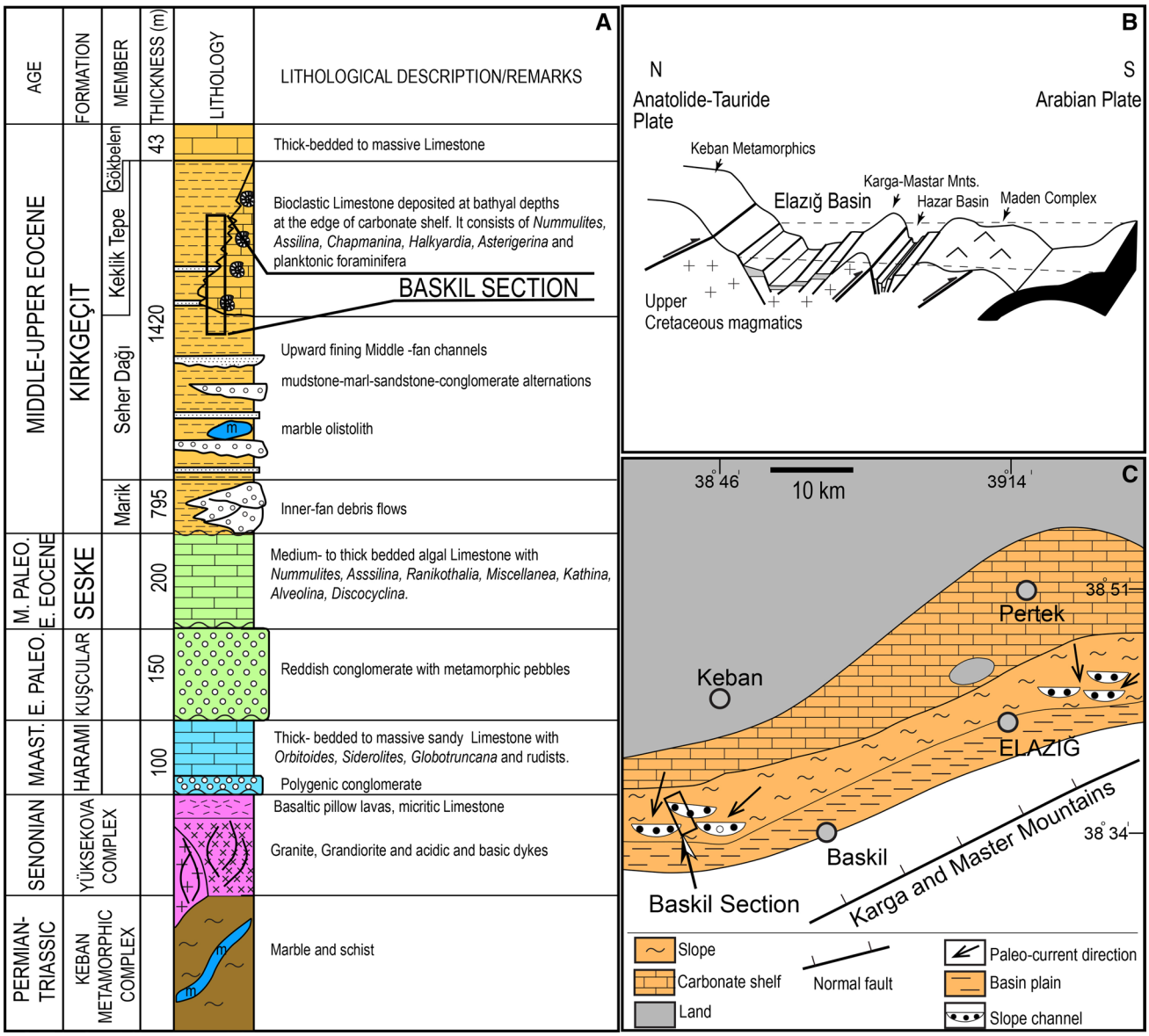

Fig. 2 **a** Generalized stratigraphy of the Baskil region and position of the Baskil section (Özkul 1988). **b** Cartoon showing the paleogeography of the Kırkgeçit Formation in the middle Eocene (Yazgan 1984; Cronin et al. 2000). **c** Paleogeographic map of the region during the middle-late Eocene (Aksoy et al. 2005)

Geological setting and general stratigraphy

The Baskil section is situated in the western part of the Elazığ Basin in eastern Anatolia, where the basin fill is exposed in a SW–NE belt extending from east of Elazığ to Malatya region (Fig. 1a). The present-day plate boundary of the Arabian and Eurasian plates, determined by the Bitlis–Zagros Suture Zone, lies to the south of the study area (Fig. 1b). The Elazığ Basin, located to the north of this suture zone, is interpreted as a marine to non-marine Cenozoic basin that evolved from a Paleocene-early Miocene back arc setting to a collisional stage in the Miocene (Aktaş and Robertson 1984; Yazgan 1984; Bingöl 1984; Özkul 1988; Cronin et al. 2000; Aksoy et al. 2005) (Fig. 2). The generalized stratigraphy of the Baskil region is described as follows (Fig. 2).

– Keban metamorphic complex and Yüksekova (Elazığ) magmatic complex: the basement of the upper Cretaceous–Paleogene basin in the Baskil region consists of the Permian–Triassic Keban metamorphics complex and the upper Cretaceous Yüksekova (or Elazığ) magmatic complex. The Keban metamorphic complex consists of marbles, calc-phyllites, calc-schists and metaconglom-

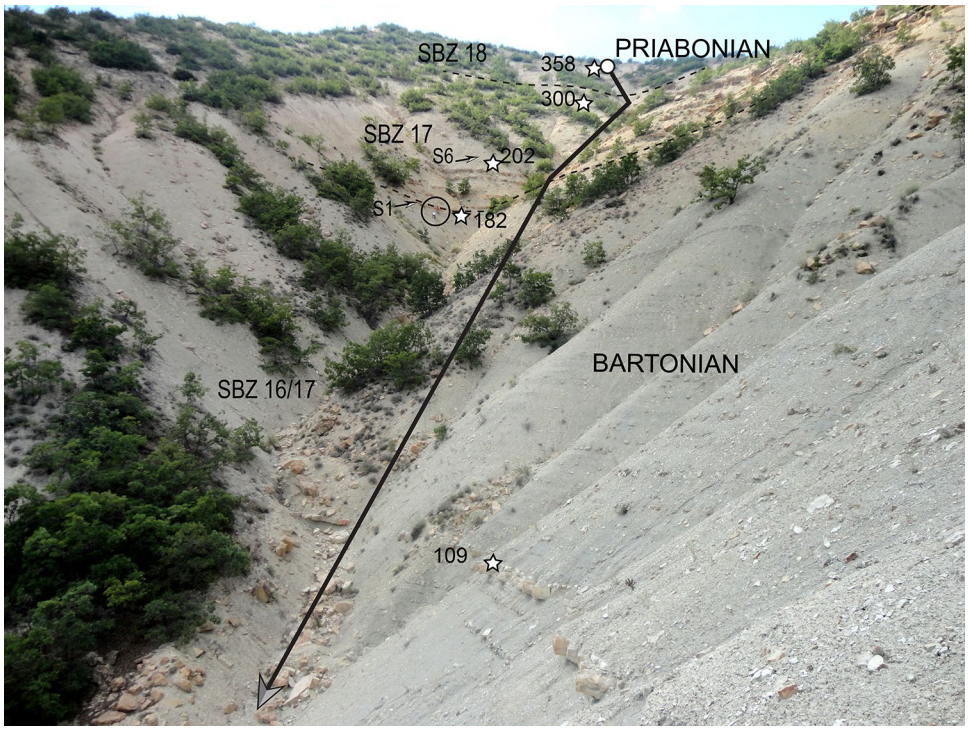

Fig. 3 View of the middle and upper part of the Baskil section and corresponding SBZ zones based on the platform-derived allochthonous LBF assemblages (M.G and R.S as a scale at the bottom of 6-sisters). Positions of some selected samples (numbers with stars) are shown

erates, which have undergone amphibolite-greenschist facies metamorphism (see Aksoy et al. 2005 and references therein). The upper Cretaceous magmatic complex consists of basalts, andesites, microdiorites and dolerites and plutonic rocks.

– Upper Cretaceous–Paleogene cover units: the Harami Formation is stratigraphically the lowest unit covering the basement rocks consisting of a basal conglomerate and overlying shallow-marine limestone (Fig. 2a). The age of the unit with larger benthic foraminifera such as *Orbitoides*, *Lepidorbitoides*, *Omphalocyclus*, *Siderolites* and rudists, is commonly accepted as (late) Maastrichtian (Yazgan 1984; Bingöl 1984; Turan 1984; Türkmen et al. 2001). The upper age range of the unit has been lately extended into middle Paleocene by Herece and Acar (2016) who recorded a Selandian foraminiferal fauna including *Sistanites, Cuvillierina,* and *Miscellanea* further to east of the study area. The lower Paleocene conglomerates of the Kuşcular Formation rest unconformably on the Harami Formation, and are unconformably overlain by a prominent carbonate unit, the Seske Formation. The latter consists of shallow-marine limestone containing late Paleocene-early Eocene foraminiferal assemblages of nummulitids, miscellaneids, and orthophragminids (Türkmen et al. 2001). The upper age range of this unit has been recently extended into the middle Eocene by Herece and Acar (2016). The Kırkgeçit Formation, a thick siliciclastic-carbonate unit indicating a significant subsidence in the basin, is a widespread unit in eastern Turkey, with the type-locality situated near the city of Van, ca. 400 km to the east of Baskil. This unit has variable facies in the Elazığ Basin, ranging from shallow-marine limestone and clastic rocks to bathyal bioclastic limestone and marls, and deeper marine siliciclastic rocks (Özkul 1988; Türkmen et al. 1999, 2001; Özcan et al. 2006; Herece and Acar 2016) (Fig. 2c). The most expanded outcrops of the Kırkgeçit Formation are more than 2 km thick, and occur to the west of the Baskil town, where four distinct members are identified (Fig. 2a).

– Marik Member, 795-m-thick lower conglomeratic unit (inner-fan conglomerates of Özkul 1988 and slope basin basal apron fill deposits of Cronin et al. 2000):
– Seher Dağı Member, ca. 1420-m-thick (including the thickness of its lateral equivalent Keklik Tepe Member) unit composed of deep-marine mudstone, marl, sandstone and conglomerate intercalations laterally passing into the bioclastic limestone beds of the Keklik Tepe Member with abundant LBF. According to Özkul (1988) and Cronin et al. (2000), the conglomerates represent the deposition in mid-fan channels (slope-channels).
– Keklik Tepe Member, a bathyal bioclastic limestone with abundant allochthonous LBF, intercalated with marls containing pelagic fauna and flora. The Seher Tepe and Keklik Tepe members are laterally interfingering.

– Gökbelen Member, a thick-bedded to massive shallow-marine limestone with limited outcrops in the study area.

In this context, according to previous studies, the Baskil section corresponds to part of the Seher Dağı and Keklik Tepe members, suggesting a deposition at bathyal depths for most of the section (Fig. 2c). The age of the Kırkgeçit Formation has been variously reported and its upper age is uncertain. The various ages ranging from middle Eocene (Lutetian) to Priabonian (Bingöl 1984; Avşar 1991, 1996) or from middle Eocene to Oligocene (Özkul 1988; Cronin et al. 2000) were assigned to the unit mostly based on LBF. Although the presence of Oligocene beds is uncertain in the Baskil region, elsewhere in the basin they occur in shallow to deep-marine facies (Hüsing et al. 2009; Herece and Acar 2016). In the study area, the Kırkgeçit Formation is unconformably overlain by the lower Miocene Alibonca Formation, which is the youngest marine unit in the Baskil area.

Baskil section: lithology and paleontological context

The Baskil section is located about 19.8 km NW of the town of Baskil in Elazığ province, eastern Turkey (Fig. 1a). The section was sampled near the main road from Baskil to Aydınlar (beginning of the section: 38°36′21.35″N, 38°36′1.38″E; end of the section: 38°36′31.56″N, 38°36′31.56″E) to the west of the Resulkahya village, where the Kırkgeçit Formation is exposed along the cliffs of the Seher Mountain (Figs. 1b, 3). The section encompasses 387 m of the Kırkgeçit Formation and corresponds to the Keklik Tepe Member of Özkul (1988) (Figs. 2a, 3). The Baskil section is composed of hemipelagic and turbidite deposits and debris flows with abundant LBF, studied at 17 levels throughout the section (Fig. 4). The key datum planes based on calcareous nannofossils, planktonic foraminifera, and LBF are presented in Table 1.

The lower part of the Baskil section (0–182 m) contains massive marls and turbiditic siltstone and sandstone beds (Fig. 5a). This part of the section is devoid of coarse turbidites and debris flow deposits and also LBF, except for sample 78, the stratigraphically lowest sample. The lowest occurrence (LO) of *Orbulinoides beckmanni* is marked at 145 m in the upper part of the section.

A 25-m-thick turbiditic section (named six sisters, S1-6 herein) between 182 and 207 m consists of intercalation of hemipelagic marls and turbidites/debris flows with abundant LBF (Fig. 5b). The highest occurrence (HO) of *O. beckmanni* at 191 m is within this turbiditic part, which contains LBF in 6 distinct levels (S1–S6). The boundary between SBZ16/17 and 17 is tentatively placed at 182 m after recording the first occurrence of taxa such as *Nummulites garganicus* Tellini, 1980 and *Operculina* ex gr. *gomezi* Colom & Bauzà within the beds just above this level.

This is followed by a succession of marls, turbidites, and debris flows (Fig. 5c–e). The HOs of *Chiasmolithus solitus* at 269 m and of *Sphenolithus obtusus* at 282 m are recognized in this part. The SBZ17/18 boundary is tentatively placed at a level above 300 m and below 314 m based on the LOs of *Nummulites hormoensis* Nuttall & Brighton, 1931 at 314 m and *H. armenica* (Grigoryan, 1986) at 323 m. The SBZ17/18 boundary stays below the Bartonian/Priabonian boundary, which is established by the LO datum of *Chiasmolithus oamaruensis* at 342 m.

The upper part of the Baskil section consists of massive marls with thick debris flow deposits and turbidites (Fig. 5f) with characteristic Priabonian LBF. This interval is characterized by the occurrence of *N. hormoensis* Nuttall & Brighton, 1931, *H. armenica* (Grigoryan, 1986), *Chapmanina gassinensis* (Silvestri, 1905) and *Silvestriella tetraedra* (Gümbel, 1868).

Results

Paleomagnetism

Throughout alternated field demagnetization, stable paleomagnetic behavior permitted to recognize reliable characteristic remanent magnetization, which defined the geomagnetic polarity. The magnetic polarity record recognized by Rodelli et al. (2018) subdivided the studied section into 12 magnetozones, of which six are reverse polarity and six normal polarity intervals. The position of the chrons boundary is precisely pinpointed along the section as reported in Table 1. Due to the continuous, undisturbed, and undeformed sedimentary record, using the ages of the geomagnetic reversals and fossil assemblages, Rodelli et al. (2018) established a detailed age model, which spans from the upper part of Subchron C19n.1r to the base of Subchron C17n.1n (42.4–37.8 Ma).

Calcareous nannofossils

About 360 m of section were sampled for calcareous nannofossils study. The samples were prepared from unprocessed material as smear slides following standard procedure and observed under a light microscope at 1250X magnification using principle transmitted light techniques. The relative number of key calcareous nannofossils was evaluated through counting methods. The percentages of *Reticulofenestra umbilicus*, *Cribrocentrum reticulatum*, *Dictyococcites bisectus* and *Cribrocentrum erbae* were obtained counting 300 specimens of the total assemblage; the percentages of

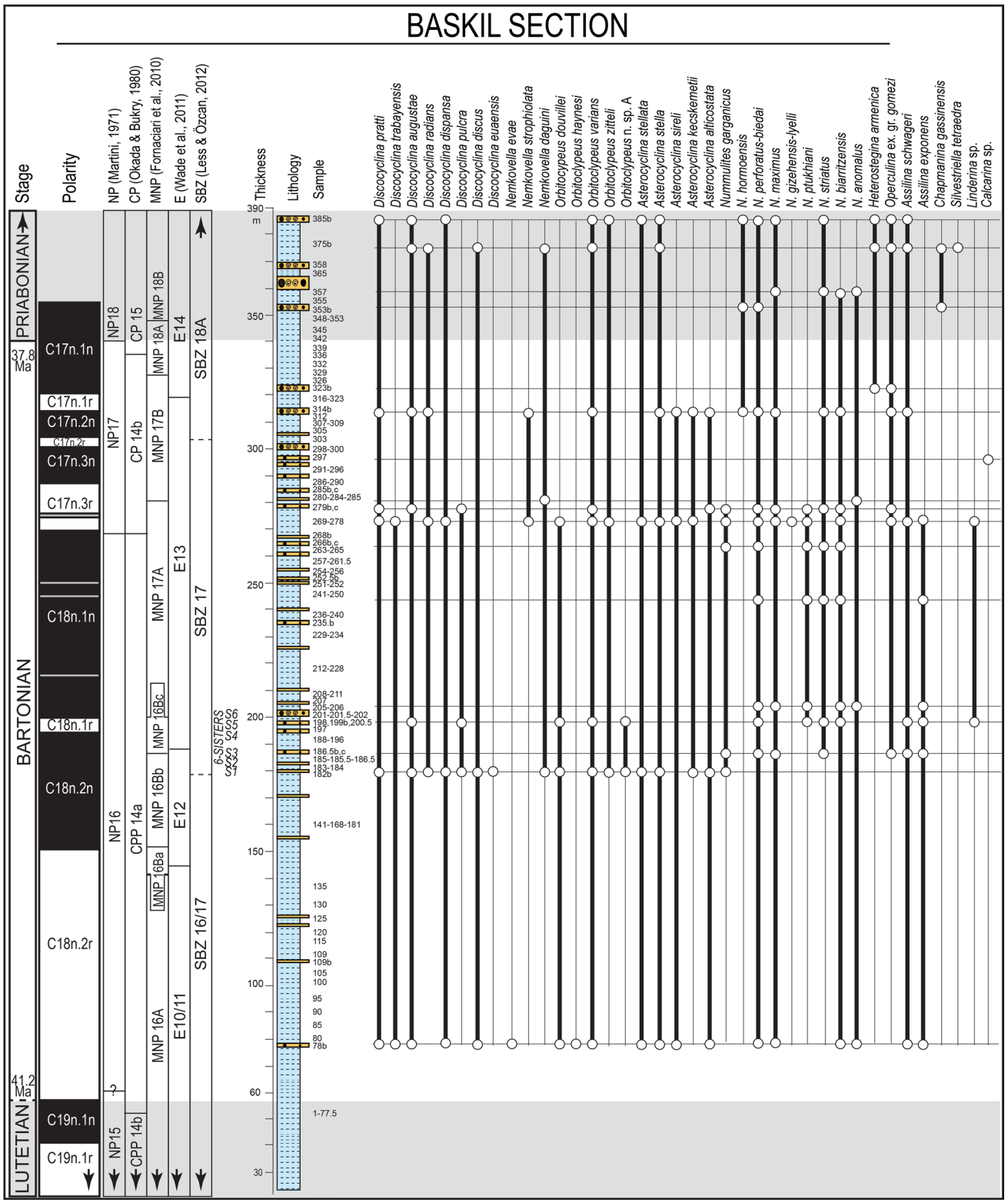

Fig. 4 Distribution of LBF and corresponding SBZ zones in Baskil section (after Serra-Kiel et al. 1998; Less and Özcan 2012), their correlation to calcareous nannofossils (NP, CP and MNP after, Martini 1971; Okada and Bukry 1980; Fornaciari et al. 2010), planktonic foraminifera (E after Wade et al. 2011) and magnetostratigraphy (after Rodelli et al. 2018). Chronostratigraphy is after Gradstein et al. (2012)

Table 1 Bioevents, and Chron boundaries, with their numerical ages for the Baskil section

Biostratigraphic event and Chron	m	NP	CP	MNP	CNE	P	E	SBZ	Gradstein et al. (2012) age (Ma)	Baskil (Ma)
AE *C. erbae*	348.0			MNP18A/MNP18B	CNE17/CNE18				–	37.40
LO *Ch. oamaruensis*	342.0	NP17/NP18							37.80	–
HO *Ch. grandis*	336.0		CP14b/CP15a						37.20	37.20
AB *C. erbae*	332.0			MNP17B/MNP18A	CNE16/CNE17				37.60	37.90
LO Heterostegina	321.0							SBZ17/SBZ18A	38.40	38.20
HO M. crassatus	321.0						E13/E14		38.10	37.90
C17n.1r/C17n.1n	320.6								37.79	–
C17n.2n/C17n.1r	313.7								37.91	–
C17n.2r/C17n.2n	305.8								38.14	–
C17n.3n/C17n.2r	301.3								38.20	–
C17n.3r/C17n.3n	285.1								38.38	–
HO *S. obtusus*	282.0			MNP17A/MNP17B	CNE15/CNE16				39.60	39.50
HO *Ch. solitus*	269.0	NP16/NP17							40.40	38.50
C18n.1n/C17n.3r	268.3								38.67	–
LO *S. obtusus*	200.5			MNP16Bc/MNP17A					39.60	39.50
C18n.1r/C18n.1n	199.8								39.69	–
C18n.2n/C18n.1r	193.0								39.76	–
HO *O. beckmanni*	191.0					P13/P14	E12/E13		40.00	39.70
HO *S. spiniger*	190.0			MNP16Bb/MNP16Bc					40.10	39.70
LO *D. bisectus*	154.0			MNP16Ba/MNP16Bb	CNE14/CNE15				40.60	40.10
C18n.2n/C18n.2r	153.4								40.20	–
LO *O. beckmanni*	145.0					P12/P13	E11/E12		40.50	40.20
HCO *S. furcatolithoides*	141.0			MNP16A/MNP16Ba					40.70	40.20
HO? *B. gladius*	61.0	NP15/NP16							43.30	41.10
C19n.1n/C18n.2n	58.1								41.20	–
LCO *C. reticulatum*	50.0				CNE13/CNE14				–	41.20
C19n.1r/C19n.1n	43.3								41.44	–
HO *D. bifax*	42.0		CP14a/CP14b						40.40	41.40

Calcareous nannofossil Zones and Subzones are after Martini (1971) (codified as NP), Okada and Bukry (1980) (codified as CP), Fornaciari et al. (2010) (codified as MNP) and Agnini et al. (2014) (codified as CNE). Planktonic foraminiferal Zones are after Wade et al. (2011) (codified as E and P). Larger benthic foraminiferal Zones and Subzones are after Serra-Kiel et al. (1998) and Less and Özcan, 2012). Chronostratigraphy is after Gradstein et al. (2012). The ages in the section were calculated using linear interpolation between magnetostratigraphy tie points of Rodelli et al. (2018)

AB, acme beginning (defined on abundance > 10%); AE, acme ending (defined on abundance < 10%); LO, occurrence; HO, highest occurrence; LCO, lowest common occurrence; HCO, highest common occurrence

Fig. 5 Field aspects of the Kırkgeçit Formation in the studied section and position of some selected samples (numbers with stars) showing important paleontological datum planes and boundaries. S1–6: 6-sisters

Sphenolithus furcatolithoides, *S. spiniger* and *S. obtusus* were evaluated counting 100 taxonomically related forms; the number of the less frequent *Discoaster bifax*, *Nannotetrina cristata*, *Blackites gladius*, *Chiasmolithus solitus*, *C. grandis* and *C. oamaruensis* was counted on 300 fields of view (roughly corresponding to 6 mm^2). The distribution of calcareous nannofossil index species is shown in Fig. 6, and microphotographs are shown in Fig. 7. The Baskil section

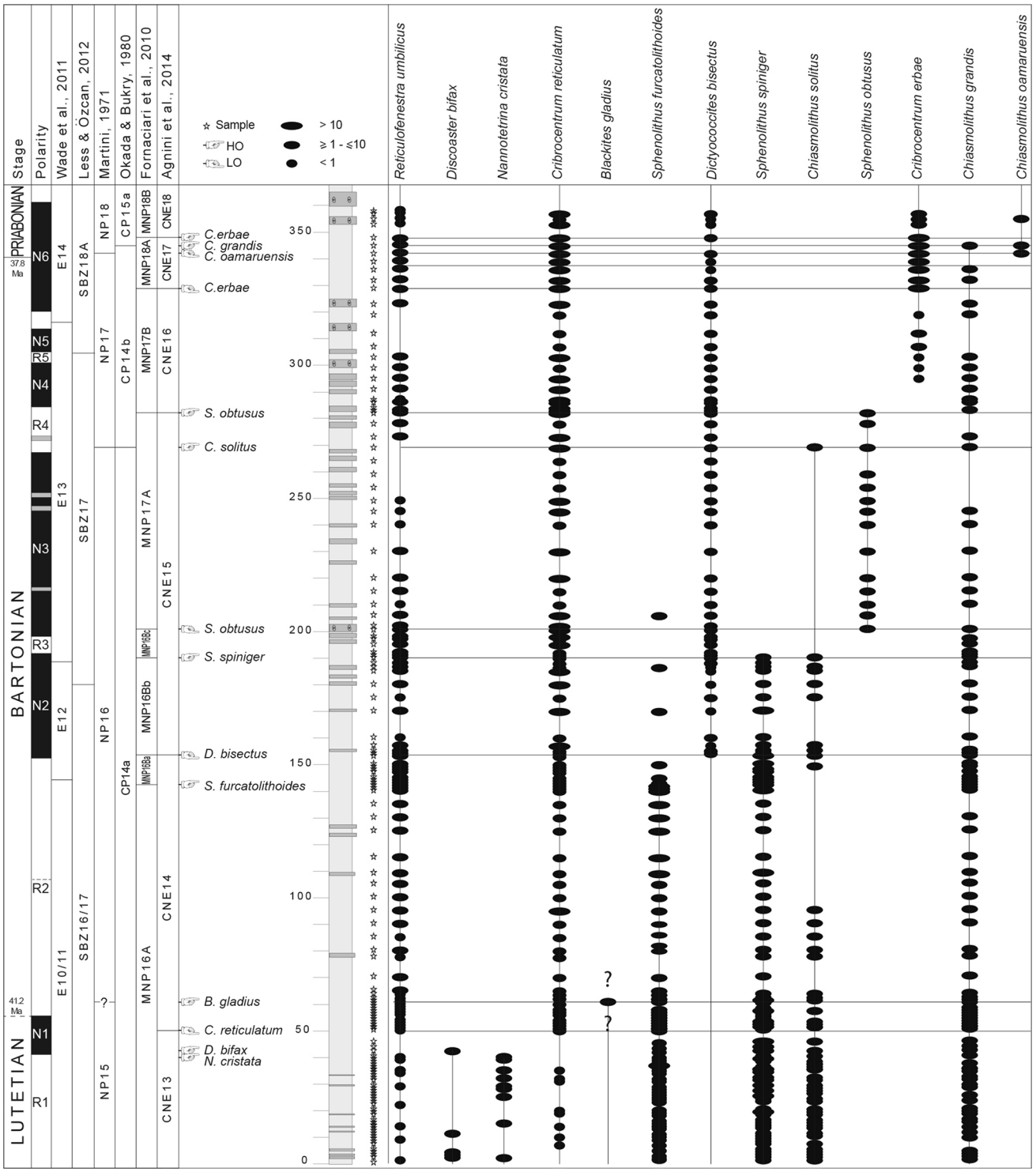

Fig. 6 Range chart of calcareous nannofossil index species from the Baskil section. LO (lowest occurrence), HO (highest occurrence). Numbers express the frequency of index species both as percentage (*R. umbilicus*, *C. reticulatum*, *D. bisectus*, *C. erbae*, *S. furcatolithoides*, *S. spiniger*, *S. obtusus*) and number in an area of 6 mm^2 (*D. bifax*, *N. cristata*, *B. gladius*, *C. solitus*, *C. grandis*, *C. oamaruensis*)

spans the Bartonian to lowermost Priabonian, for this interval of time the biostratigraphic MNP scheme of Fornaciari et al. (2010) and CNE scheme of Agnini et al. (2014) were also adopted for improving the time resolution of the standard NP scheme of Martini (1971) and the CP scheme of Okada and Bukry (1980).

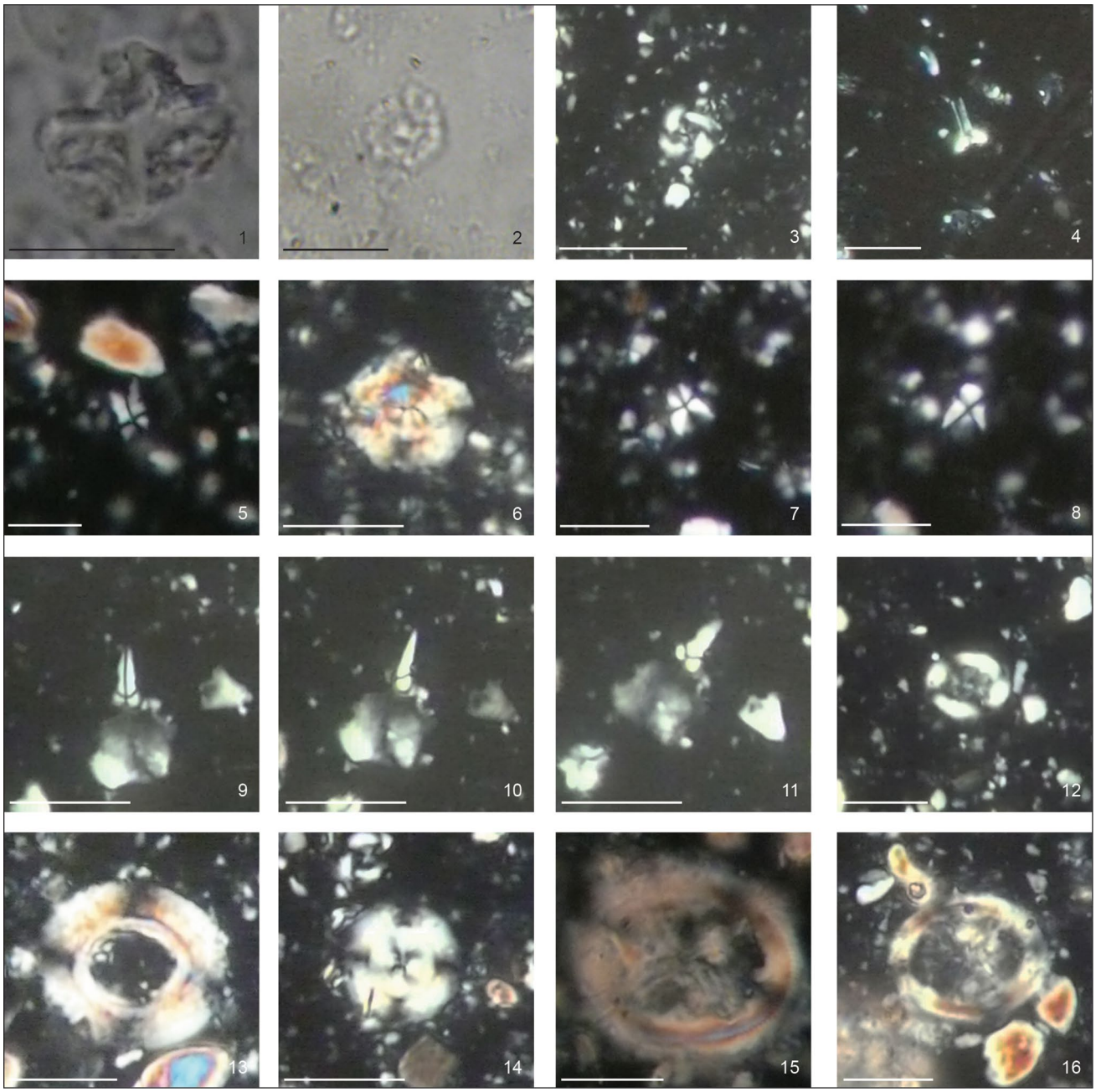

Fig. 7 Microphotographs of calcareous nannofossil index species from the Baskil section. **1** *Nannotetrina cristata* (Martini, 1958) Perch-Nielsen 1971, parallel nicols, sample 25. **2** *Discoaster bifax* Bukry, 1971, parallel nicols, sample 2. **3** *Cribrocentrum reticulatum* (Gartner & Smith 1967) Perch-Nielsen 1971, crossed nicols, sample 269. **4** *Blackites gladius* (Locker, 1967) Varol 1989, crossed nicols, sample 61. **5** *Sphenolithus furcatolithoides* Locker 1967, crossed nicols, sample 109. **6** *Dictyococcites bisectus* (Hay et al. 1966) Bukry and Percival 1971, crossed nicols, sample 269. **7** *Sphenolithus spiniger* Bukry 1971, 0°, crossed nicols, sample 140. **8** *Sphenolithus spiniger* Bukry 1971, 45°, crossed nicols, sample 140. **9** *Sphenolithus obtusus* Bukry 1971, 0°, crossed nicols, Sample 269. **10** *Sphenolithus obtusus* Bukry 1971, 22°, crossed nicols, sample 269. **11** *Sphenolithus obtusus* Bukry 1971, 45°, crossed nicols, sample 269. **12** *Chiasmolithus solitus* (Bramlette and Sullivan 1971) Locker 1968, crossed nicols, sample 37. **13** *Reticulofenestra umbilicus* (Levin 1965) Martini and Ritzkowski 1968, crossed nicols, sample 345. **14** *Cribrocentrum erbae* Fornaciari et al. in Fornaciari et al. 2010, crossed nicols, sample 345. **15** *Chiasmolithus grandis* (Bramlette & Riedel 1954) Radomski 1968, crossed nicols, sample 345. **16** *Chiasmolithus oamaruensis* (Deflandre, 1954) Hay et al. 1966, crossed nicols, sample 345. Scale bar 10 μm

The following bioevents and Zones–Subzones were identified as shown in Fig. 6. The standard bioevents are the LO of *C. oamaruensis* that was detected at 342 m and easily allows the identification of the base of Zone NP18, and the HO of *C. solitus*, that was detected at 269 m and defines the base of Zone NP17 and the base of Subzone CP14b. The HO of *C. grandis* was detected at 345 m, after additional counting, and identifies the CP14b–CP15a boundary, whereas the HO of *B. gladius* seems to be unreliable as the species was observed only at 61 m, so that the position of the base of Zone NP16 is uncertain. Considering the more recent biozonations, the LO of common *C. reticulatum* was observed at 50 m and defines the base of Zone CNE14, the HO of common *S. furcatolithoides* was recognized at 142 m and sets the base of Subzone MNP16Ba, the LO of *D. bisectus* was detected at 154 m and defines the base of Subzone MNP16Bb and Zone CNE15, the HO of *S. spiniger* was observed at 190 m and identifies the MNP16Bb–MNP16Bc boundary. The total range of *S. obtusus*, recorded between 200.5 and 282 m, allows the recognition of Zone MNP17A, and its HO indicates the CNE15–CNE16 boundary. The LO and HO of the high abundance interval of *C. erbae*, recorded between 332 and 348 m, identify Zone MNP18A and Zone CNE17, the sharp decrease of abundance of *C. erbae* is also used to define the base of Zone MNP18B and Zone CNE18.

Foraminifera

Samples for planktonic foraminiferal biostratigraphy and benthic foraminiferal quantitative analyses were treated following the cold acetolysis technique of Lirer (2000) by sieving through a 63 µm mesh and drying at 50 °C. The so-obtained residues were studied with a binocular microscope to identify planktonic foraminiferal biostratigraphic marker species and to characterize the benthic foraminiferal assemblages. The planktonic foraminiferal standard zonation scheme of Wade et al. (2011) was followed. A total of 116 and 31 samples were processed for planktonic and benthic foraminifera, respectively. For benthic foraminifera, at least 300 specimens were picked from the fraction greater than 125 µm.

Planktonic foraminifera

Planktonic foraminifera are generally abundant and well diversified with moderate to good state of preservation. They are represented by typical middle-late Eocene low-latitude taxa, with different species of the genera *Acarinina*, *Catapsydrax*, *Dentoglobigerina*, *Globigerina*, *Globigerinatheka*, *Globorotaloides*, *Globoturborotalia*, *Guembelitrioides*, *Morozovelloides*, *Orbulinoides*, *Paragloborotalia*, *Parasubbotina*, *Planorotalites*, *Subbotina* and *Turborotalia*. The main biostratigraphical events are (from bottom to top): (1) the LO of *O. beckmanni* at 145 m; (2) the HO of *O. beckmanni* at 191 m; and (3) HO of *Morozovelloides crassatus* at 321 m (Rodelli et al. 2018) (Fig. 8). On the basis of these bioevents, the Baskil section spans from the E10/E11 to E14 planktonic foraminiferal Zones of Wade et al. (2011) (Fig. 4 and Table 1).

Smaller benthic foraminifera

Smaller benthic foraminifera are abundant and highly diversified throughout the study interval of the Baskil section. Although the state of preservation is poor in the 160–180 m interval corresponding to the Middle Eocene Climatic Optimum, elsewhere in the section the preservation is good. A total of 224 species belonging to 111 genera were identified. The assemblages are dominated by calcareous taxa whereas agglutinated and porcelaneous forms represent only a minor part. *Anomalinoides*, *Bathysiphon*, *Bulimina*, *Cibicidoides*, *Lagena*, *Lenticulina*, *Melonis*, *Nodosaria*, *Nuttallides*, *Oridorsalis*, *Praebulimina*, *Pullenia*, *Stilostomella*, and *Uvigerina* are the dominant genera. The most abundant calcareous taxa are *Lenticulina* sp. (5.9%), *Nodosaria* sp. (5.5%), *Lagena* sp. (5.2%), *Nuttallides truempyi* (3.1%), *Laevidentalina* sp. (2.4%), *Gyroidinoides beisseli* (2%), *Cibicidoides eocaenus* (1.8%), *Cibicidoides* sp. (1.6%), *Nuttallides* sp. (1.5%), *Gyroidinoides* sp. (1.4%), *Cibicides* sp. (1.3%), *Stilostomella* sp. (1.3%), *Hanzawaia ammophila* (1.1%), *Bulimina alazanensis* (1.1%), *Anomalinoides* sp. (1%), *Uvigerina* sp. (1%), and *Gyroidinoides globosus* (1%), *Melonis* sp. (0.9%) and *Oridorsalis umbonatus* (0.9%). The agglutinated species are mainly represented by *Bathysiphon* sp. (8.5%), *Dorothia* sp. (1.4%), *Rhabdammina* sp. (1.2%), and *Hormosina* sp. (1%). Porcelaneous species are rare and mainly include *Quinqueloculina* sp. (0.1%) and *Sigmoilopsis* sp. (0.1%). Several diagnostic taxa with an upper depth limit in the upper bathyal are recognized, namely *Anomalinoides alazanensis*, *Anomalinoides capitatus*, *B. alazanensis*, *B. jacksonensis*, *B. tuxpamensis*, *Cibicidoides bradyi*, *Cibicidoides eocaenus*, *C. mexicanus, C. micrus*, *H. ammophila*, *Osangularia plummerae*, *Planulina ambigua*, *Spiroplectammina spectabilis*, *Uvigerina rippensis*, *Uvigerina spinulosa*, *N. truempyi* and *Globocassidulina subglobosa* (Fig. 9). On the basis of the dominance of calcareous tests, the state of preservation, and the upper depth limit of diagnostic taxa, the section was likely deposited at an upper bathyal (~ 300–600 m) environment (Rodelli et al. 2018).

Larger benthic foraminifera

In Baskil section, LBF are dominated by orthophragminids and nummulitids with sparse rotaliids. Taxa listed in the Appendix 'List of larger benthic foraminifera from the Baskil section' were identified. Their assemblages suggest

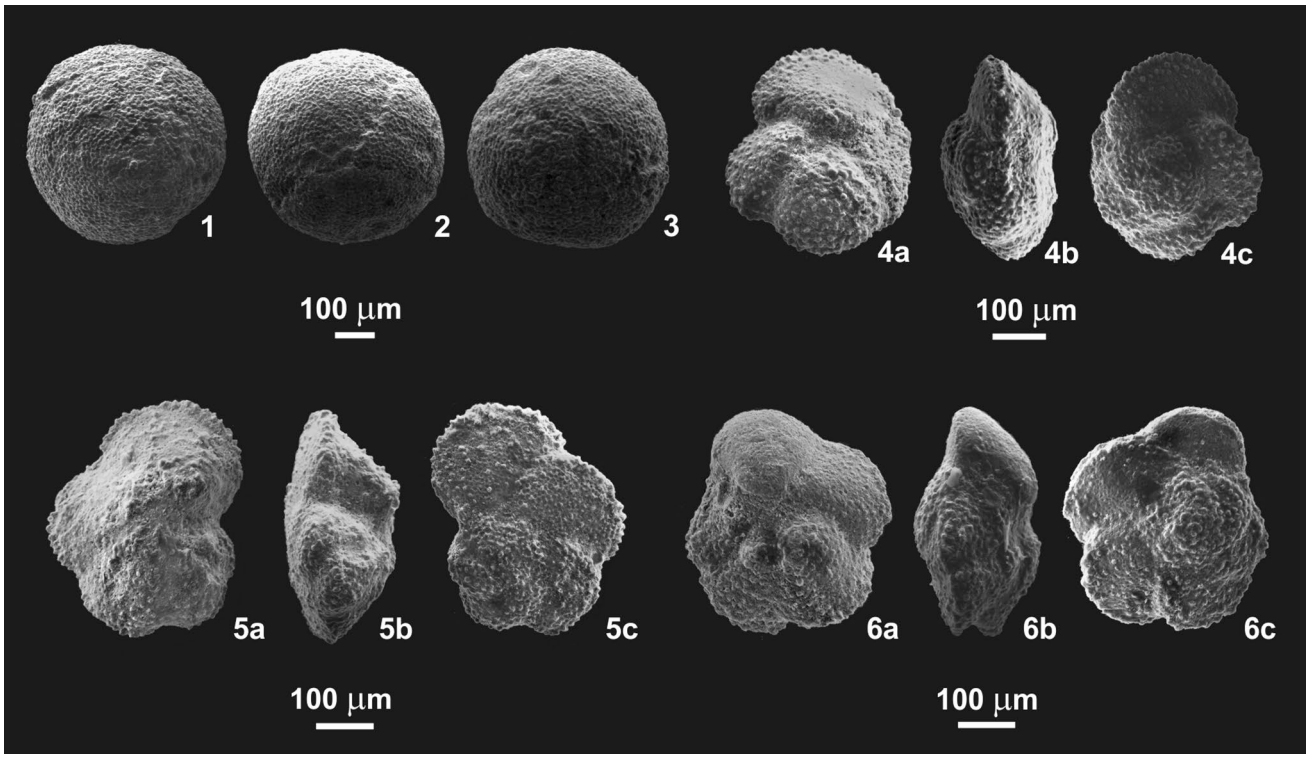

Fig. 8 Microphotographs of index planktonic foraminifera from the Baskil section. **1–3** *Orbulinoides beckmanni* (Saito, 1962), sample 177. **4a–c** *Morozovelloides crassatus* (Cushman, 1925), sample 275. **5a–c** *Morozovelloides crassatus* (Cushman, 1925), sample 270. **6a–c** *Morozovelloides crassatus* (Cushman, 1925), sample 275

SBZ16/17 (OZ12), 17 (OZ13) and 18A (OZ14) throughout the section (Fig. 4).

The stratigraphically lowest level with LBF (sample 78) contains the species/subspecies of the following orthophragminid and nummulitid taxa; *Discocyclina pratti pratti, D. trabayensis trabayensis, D. augustae olianae*, *D. dispansa hungarica, D. discus, N. evae* cf. *reinechensis, Orbitoclypeus douvillei pannonicus, O. haynesi, O. varians scalaris, Asterocyclina stellata stellata, A. stella stella, A. sireli, A. alticostata cuvillieri, Nummulites perforatus-biedai, N. maximus, N. biarritzensis, N. anomalus, A. schwageri,* and *A. exponens*. This sample is just above the Lutetian and Bartonian boundary and the assemblage characterizes the lower Bartonian (Fig. 4). Based on the presence of *Orbitoclypeus douvillei pannonicus*, *O. varians scalaris* and *Asterocyclina alticostata cuvillieri* the assemblage of the above taxa is characteristic for the SBZ16/17, and in terms of the orthophragminid zonation by Less (1998a) for the OZ12 Zone. This interval is tied to C18n.2r, and stays within NP16, MNP16A, and E10/E11 zones.

The interval between 182 and 207 m (herein informally referred to as 'six sisters') yielded *Discocyclina pratti pratti, D. augustae olianae*, *D. radians* cf. *labatlanensis*, *D. dispansa dispansa, D. pulcra balatonica*, *D. discus*, *D. euaensis*, *Orbitoclypeus douvillei malatyaensis, O. varians varians, O. zitteli*, *Orbitoclypeus* n. sp. A, *Asterocyclina stellata stellata, A. stella stella, A. kecskemetii*, *Asterocyclina alticostata alticostata, N. garganicus*, *Nummulites perforatus-biedai, N. maximus, Nummulites ptukhiani*, *N. striatus*, *N. biarritzensis, N. anomalus, Operculina* ex gr. *gomezi*, *A. schwageri, A. exponens* and *Linderina* sp. Based on the presence of *Orbitoclypeus douvillei malatyaensis*, *O. varians varians, A. alticostata alticostata* and *N. garganicus*, the assemblages of the above taxa are characteristic for SBZ17, and in terms of the orthophragminid zonation for OZ13 Zone. This interval is correlated with the *O. beckmanni* Zone (E12) and lower part of E13, implying a Bartonian age (Fig. 4).

The section between 207 and 250 m is dominated by marls and turbidites with sporadic LBF. Sample 242 in the upper part yielded only nummulitids such as *Nummulites perforatus-biedai, N. ptukhiani*, *N. striatus*, *N. biarritzensis,* and *A. exponens*. Marls and turbidites between 265 and 290 m yielded a diverse LBF represented by *Discocyclina pratti pratti, D. trabayensis elazigensis, D. augustae*, *D. radians* cf. *labatlanensis*, *D. dispansa sella, D. pulcra* cf. *balatonica*, *Nemkovella strophiolata* n. ssp. Padragkút, *Orbitoclypeus douvillei malatyaensis, O. varians varians, O. zitteli*, *Asterocyclina stellata stellata, A. stella stella*, *A. sireli, A. kecskemetii*, *A. alticostata alticostata, N. garganicus*,

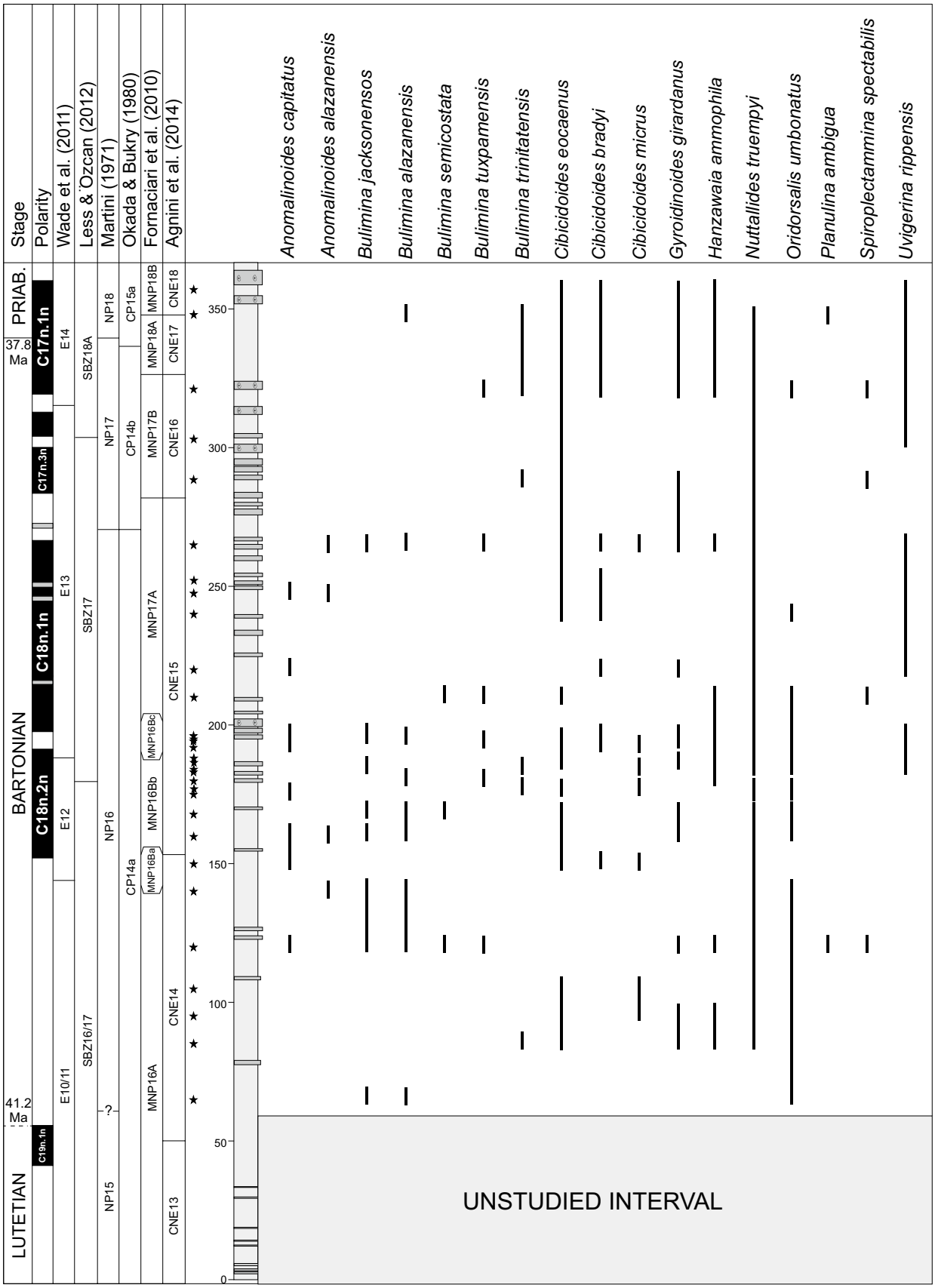

Fig. 9 Distribution of smaller benthic foraminifera in Baskil section

Nummulites perforatus—biedai, N. maximus, N. gizehensis-lyelli, *N. ptukhiani*, *N. striatus*, *N. biarritzensis, N. anomalus, Operculina* ex. gr. *gomezi*, *A. schwageri* and *Linderina* sp. The assemblages of above taxa are basically identical with those from the 6-sisters and also characteristic for the SBZ17 (and in terms of the orthophragminid zonation for the OZ13 Zone). This part of the section overlaps with E13, NP16 and lower part of NP17 zones and implies a Bartonian age.

The upper part of the section between 290 and 387 m yields *Discocyclina pratti, D. augustae*, *D. radians*, *D. dispansa, D. discus*, *Nemkovella strophiolata* n. ssp. Padragkút, *O. varians varians, O. zitteli*, *Asterocyclina stellata, A. stella*, *A. sireli, A. kecskemetii*, *A. alticostata alticostata, N. hormoensis*, *Nummulites perforatus-biedai, N. maximus*, *N. striatus*, *N. biarritzensis, N. anomalus, Heterostegina armenica armenica, Operculina* ex gr. *gomezi*, *A. schwageri, C. gassinensis* and *S. tetraedra*. Based on the disappearance of *N. garganicus*, *N. ptukhiani*, *Assilina exponens*, *Discocyclina pulcra* and *Orbitoclypeus douvillei* and also on the appearance of *N. hormoensis*, *H. armenica armenica*, *C. gassinensis* and *S. tetraedra*, this part belongs to the SBZ18A Zone (and to the OZ14 Zone in terms of the orthophragminid zonation), and spans NP17, lower part of NP18, upper part of E13 and E14, implying a transition from Bartonian to Priabonian (Fig. 4).

Orthophragminids

Orthophragminids in Baskil section belong to 21 lineages (Figs. 4, 11). General test features in Tethyan orthophragminid genera and parameters used in species/subspecies identification (based on Less 1998a and updated by Zakrevskaya et al. 2011; Özcan et al. 2016) are shown in Fig. 10. Brief information for each group is given below.

Discocyclina trabayensis Neumann, 1955

Discocyclina trabayensis is an unribbed species having a very small, iso- to nephrolepidine embryon, very low and relatively wide "varians"-type adauxiliary chamberlets, and narrow equatorial chamberlets with "trabayensis"-type growth pattern. This species includes tree subspecies in the Tethys: *D. trabayensis trabayensis* Neumann, 1955 (D_{mean} < 125 µm); *D. trabayensis elazigensis* Özcan & Less, 2006 (D_{mean} = 125–170 µm); *D. trabayensis vicensensis* Less, 1987 (D_{mean} > 170 µm).

This species is sparse and is characterized by *D. trabayensis trabayensis* (Fig. 12a–c) and *D. trabayensis elazigensis* in SBZ16/17 and 17, respectively (Fig. 11). *Discocyclina trabayensis* does not occur in the upper part of the section, though its stratigraphic range extends until the end of Priabonian (Less et al. 2011).

Discocyclina augustae van der Weijden, 1940

Discocyclina augustae is an unribbed species with a small, semi-iso- to nephrolepidine embryon, narrow and low "archiaci"-type adauxiliary chamberlets and also narrow and relatively low equatorial chamberlets mostly with "strophiolata"-type growth pattern. This species includes four subspecies in Tethys: *D. augustae sourbetensis* Less, 1987 (D_{mean} < 145 µm); *D. augustae atlantica* Less, 1987 (D_{mean} = 145–180 µm); *D. augustae olianae* Almela & Rios, 1942 (D_{mean} = 180–225 µm); *D. augustae augustae* van der Weijden, 1940 (D_{mean} > 225 µm).

This species occurs throughout the section and is represented by *D. augustae olianae* Almela and Rios in the lower part of the section in SBZ16/17 (Fig. 12d, e). It is rare in the upper part and no subspecific designation was made (Fig. 12f–i). *Discocyclina augustae* became extinct at SBZ20/21 boundary in the Tethys (Less and Özcan 2012).

Discocyclina dispansa (Sowerby, 1840)

Discocyclina dispansa is an unribbed species with a small- to medium-sized, semi-nephro- to trybliolepidine embryon, moderately wide and high, "archiaci"-type adauxiliary chamberlets and equatorial chamberlets. This species includes six subspecies in the Tethys: *D. dispansa broennimanni* Less, 1987 (D_{mean} < 160 µm); *D. dispansa taurica* Less, 1987 (D_{mean} = 160–230 µm); *D. dispansa hungarica* Kecskeméti, 1959 (D_{mean} = 230–290 µm); *D. dispansa sella* (d'Archiac, 1850 (D_{mean} = 290–400 µm); *D. dispansa dispansa* (Sowerby, 1840) (D_{mean} = 400–520 µm); and *D. dispansa umbilicata* (Deprat, 1905) (D_{mean} > 520 µm).

At its type-locality in Kutch (W India), this species is invariably represented by flat forms (Özcan et al. 2018). In the Western Tethys (peri-Mediterranean region and Europe), both flat and saddle-shaped forms with similar embryonic configurations but showing a wide range in embryon diameter were previously assigned to this species (Less 1987; Özcan et al. 2006, 2010). Therefore, it seems necessary to re-evaluate *D. dispansa* in the Western Tethys. This species is represented by *D. dispansa hungarica* Kecskeméti in the lower part of the section (sample 78), by *D. dispansa dispansa* (Sowerby) in the lower part of 6-sisters (sample 182), and by *D. dispansa sella* (d'Archiac) in sample 276 (Fig. 13e). Few specimens in the upper part (samples 385) were identified at species level (Fig. 13f). In the Western Tethys, *D. dispansa* became extinct at SBZ20/21 boundary (Less and Özcan, 2012).

Discocyclina pratti (Michelin, 1846)

Discocyclina pratti is an unribbed species having a medium-sized to large, tryblio- to excentrilepidine embryon,

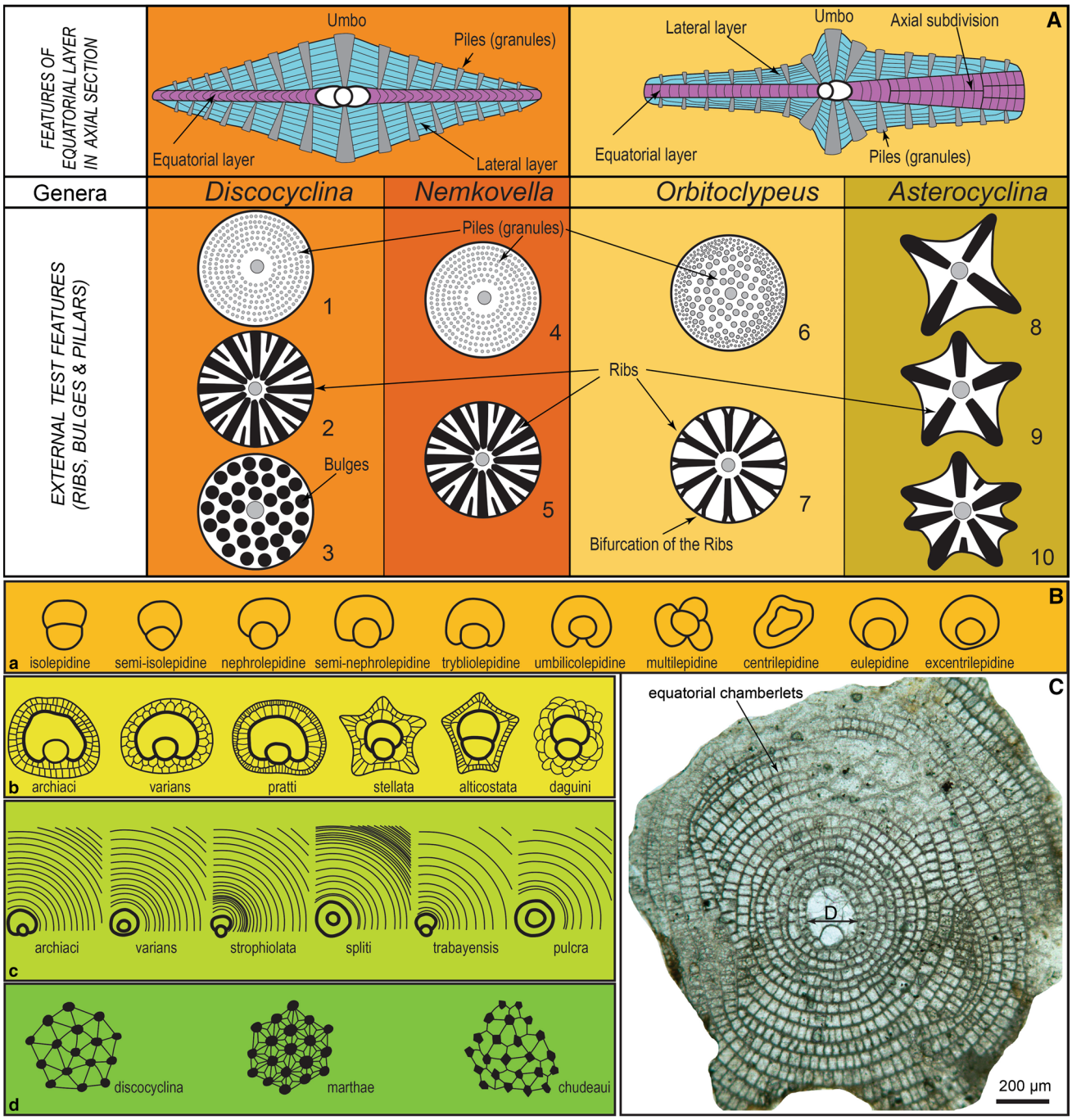

Fig. 10 General test features in Tethyan orthophragminid genera (**a**) (after Less 1987; Ferràndez-Cañadell 1997; Özcan et al. 2016), qualitative parameters (**b**): a—types of embryon configurations, b—types of the adauxiliary chamberlets, c—different growth patterns of the equatorial annuli, d—types of granules and lateral chamberlets on the test surface, and parameter D (diameter of deuteroconch) used in the morphometric description of orthophragminids as illustrated in *D. pseudodispansa* (**c**)

numerous moderately wide and high, "pratti"-type adauxiliary chamberlets and narrow but high equatorial chamberlets with "pulcra"-type growth pattern. This species is subdivided into three subspecies in the Tethys: *D. pratti montfortensis* Less, 1987 (D_{mean} < 510 µm); *D. pratti pratti* (Michelin, 1846) (D_{mean} = 510–700 µm); *D. pratti minor* Meffert, 1931 (D_{mean} > 700 µm).

Discocyclina pratti is represented by *D. pratti pratti* (Michelin) in the lower and upper part of the section (Figs. 11, 13a–c). Few specimens from the uppermost part

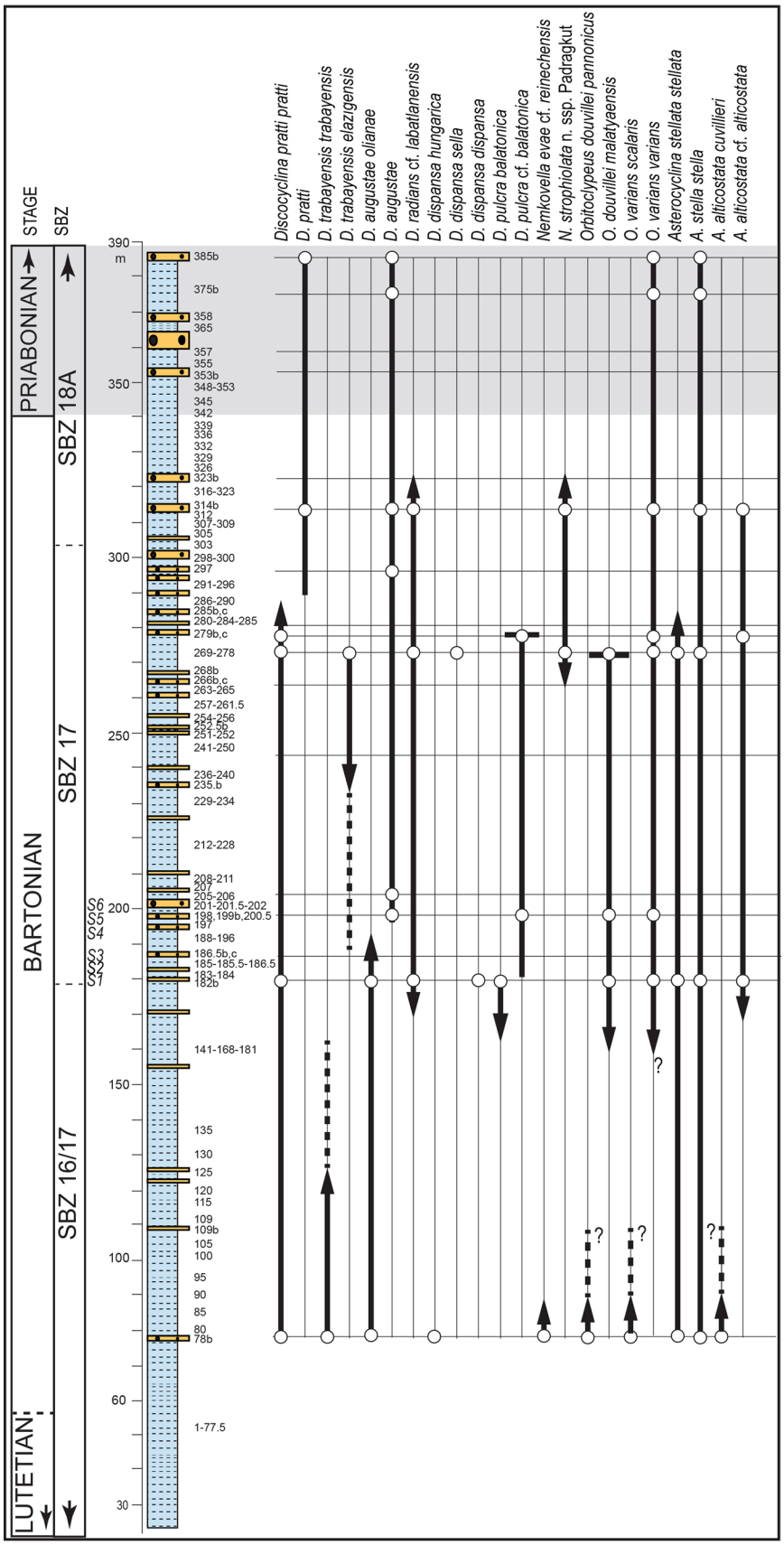

Fig. 11 Distribution of some key orthophragminid species/subspecies in the Baskil section. Dashed line shows probable occurrence. The extinction of two orthophragminid lineages (*Discocyclina pulcra* and *Orbitoclypeus douvillei*) in SBZ17 is marked

Fig. 12 Equatorial sections of *Discocyclina pratti, D. radians, D. dispansa* and *D. pulcra* from the Baskil section. **a**–**c** *D. pratti* (Michelin), **a** 78–30, **b** 182b-43, **c** 276b-10, **d** *D. radians* (d'Archiac), 276b-26, **e** *D. dispansa* (Sowerby) *sella* (d'Archiac), 276b-13, **f** *D. dispansa* (Sowerby), 385b-8, **g** *D. pulcra* (Checchia-Rispoli), 182b-33

Fig. 13 Equatorial sections of *Discocyclina trabayensis* and *D. augustae* from the Baskil section. **a–c** *D. trabayensis trabayensis* Neumann, **a** 78–61, **b** 78–59, **c** 78–33. **d**, **e**, **g**, **i** *D. augustae* van der Weijden *olianae* Almela & Rios, **d** 78–63, **e** 78–64, **g** 182b-53, **h** 78-66, **i** 182b-55. **f** *D. augustae* van der Weijden, 375b-9

were identified at species level. In the Western Tethys, *D. pratti* became extinct across the SBZ19A/B boundary before the Eocene–Oligocene boundary (Less and Özcan, 2012).

Discocyclina discus (Rütimeyer, 1850)

Discocyclina discus is a large, saddle-shaped and unribbed form with a giant, mostly umbilicolepidine (rarely also tryblio- or excentrilepidine) embryon, numerous, wide and high, 'archiaci' or transitional 'archiaci-pratti'-type adauxiliary chamberlets and wide and high equatorial chamberlets with 'archiaci' or transitional 'archiaci-pulcra'-type growth pattern. This species includes two subspecies in the Tethys: *D. discus discus* (Rütimeyer, 1850) ($D_{mean} < 1350$ µm) and *D. discus sowerbyi* Nuttall, 1926 ($D_{mean} > 1350$ µm).

This species occurs sporadically in three levels (samples 78, 182 and 375) (Figs. 11, 14a, b) not permitting subspecific identification. In the Western Tethys, *D. discus* became extinct in the Priabonian across the SBZ18/19 boundary (Less and Özcan, 2012).

Discocyclina pulcra (Checchia-Rispoli, 1909)

Discocyclina pulcra is an unribbed species having a large to giant centrilepidine embryon, numerous wide and high to very high, "pratti"-type adauxiliary chamberlets and relatively narrow but high to very high equatorial chamberlets with "pulcra"-type growth pattern. It is subdivided into five subspecies in the Tethys: *D. pulcra landesica* Less, 1987 ($D_{mean} < 800$ µm); *D. pulcra pulcra* (Checchia-Rispoli, 1909) ($D_{mean} = 800$–1000 µm); *D. pulcra* n. ssp. Angoumé Less, 1998 ($D_{mean} = 1000$–1250 µm); *D. pulcra balatonica* Less, 1987 ($D_{mean} = 1250$–1600 µm); *D. pulcra baconica* Less, 1978 ($D_{mean} > 1600$ µm).

This species occurs in three levels (samples 182, 198 and 279), assigned to *D. pulcra balatonica* in sample 182 (Fig. 13g) and *D. pulcra* cf. *balatonica* in samples 198 and 279. *Discocyclina pulcra* became extinct within SBZ17 in the Western Tethys (Less and Özcan 2012).

Discocyclina euaensis Whipple, 1932

Discocyclina euaensis is an unribbed species with a small- to medium-sized semi-nephro- to trybliolepidine embryon, wide and moderately high, "pratti"-type adauxiliary chamberlets and narrow and high equatorial chamberlets with "pulcra"-type growth pattern.

The species has not yet been subdivided into subspecies. *Discocyclina euaensis* occurs only in 6-sisters and has been previously illustrated from the coeval beds of the Kırkgeçit Formation in the same area by Özcan et al. (2006; pl. 3, Figs. 20–21).

Discocyclina radians (d'Archiac, 1850)

Discocyclina radians is a ribbed species with a small- to medium-sized semi-nephro- to trybliolepidine embryon, wide and moderately high, "pratti"-type adauxiliary chamberlets and narrow and high equatorial chamberlets with "pulcra"-type growth pattern. It includes four subspecies in the Tethys: *D. radians* n. ssp. Caupenne ($D_{mean} < 240$ µm); *D. radians noussensis* Less, 1987 ($D_{mean} = 240$–300 µm); *D. radians radian*s (d'Archiac, 1850) ($D_{mean} = 300$–375 µm); *D. radians labatlanensis* Less, 1987 ($D_{mean} > 375$ µm).

This species occurs sporadically in samples 182, 276 (Fig. 13d), 314 and 375, not permitting subspecific identification.

Nemkovella evae Less, 1987

Nemkovella evae is an unribbed species with a relatively small to moderate semi-iso- nephrolepidine embryon, low and relatively wide, very diagnostic, arcuate, "varians"-type adauxiliary chamberlets, and moderately narrow and low equatorial chamberlets with mostly "varians" and "archiaci" types of the growth pattern. It includes tree subspecies in the Tethys: *N. evae evae* Less, 1987 ($D_{mean} < 260$ µm); *N. evae karitensis* Özcan & Less, 2007 ($D_{mean} = 260$–550 µm); *N. evae reinechensis* Özcan, Ismail-Lattrache & Boukhalfa, 2014 ($D_{mean} > 550$ µm).

This species occurs only in 6-sisters, and is represented by *N. evae* cf. *reinechensis* (Fig. 14c). The upper age limit of this taxon, although not surely known, seems to be within the Bartonian (SBZ17). At its type-locality in Tunisia, this subspecies is of Bartonian age (SBZ17) (Ben Ismail-Lattrache et al. 2014).

Nemkovella strophiolata (Gümbel, 1870)

Nemkovella strophiolata is an unribbed species with a small semi-iso to nephrolepidine embryon, low and relatively wide, very diagnostic, arcuate, "varians"-type adauxiliary chamberlets, and moderately narrow and low equatorial chamberlets with "strophiolata"-type growth pattern. It includes four subspecies in the Tethys: *N. strophiolata fermonti* Less, 1987 ($D_{mean} < 150$ µm); *N. strophiolata strophiolata* (Gümbel, 1870) ($D_{mean} = 150$–185 µm); *N. strophiolata* n. ssp. Padragkút ($D_{mean} = 185$–230 µm); *N. strophiolata tenella* (Gümbel, 1870) ($D_{mean} > 230$ µm).

This species occurs in samples 276 and 314 (Fig. 14d) and is represented by *N. strophiolata* n. ssp. Padragkút. Less and Özcan (2012) reported its upper stratigraphic range in the Tethys as SBZ19A-B boundary within the Priabonian.

Nemkovella daguini (Neumann, 1958)

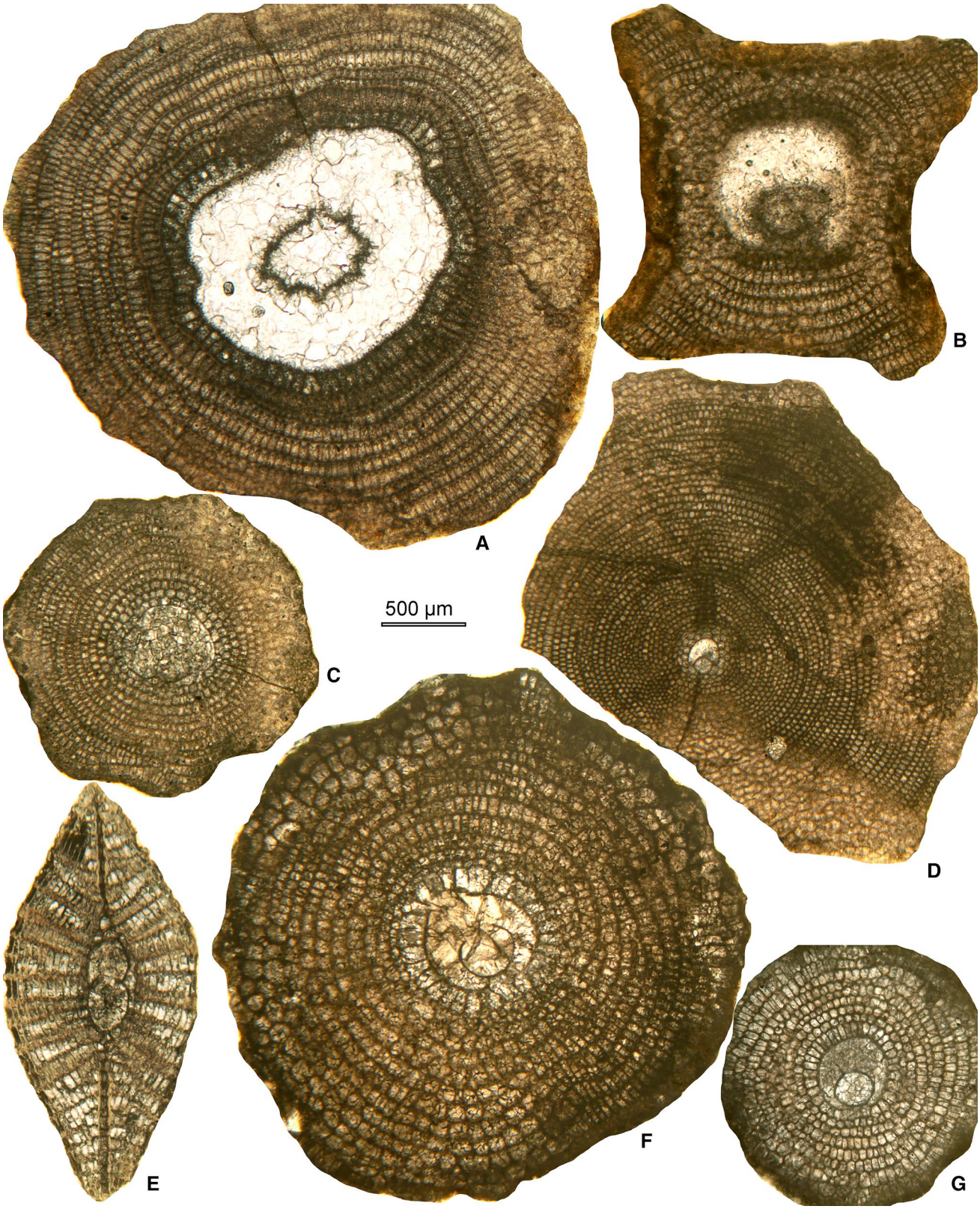

Fig. 14 Equatorial sections of *Discocyclina discus, Nemkovella evae, N. strophiolata* and equatorial and vertical sections of *Orbitoclypeus douvillei* from the Baskil section. **a**, **b** *D. discus* (Rütimeyer), **a** 78–75, **b** 375b-8, **c** *N. evae* cf. *reinechensis* Özcan, İsmail-Lattrache & Boukhalfa, 78-72, **d** *N. strophiolata* n. ssp. Padragkút, 314b-18, **e**, **g** *O. douvillei pannonicus* Less, **e** 78–45, **g** 78–41, **f** *O. douvillei malatyaensis* Özcan & Less, 182b-19. E axial, others equatorial sections

Nemkovella daguini is a small-sized, unribbed species with a very small iso- to nephrolepidine-type embryon, with few and "daguini"-type adauxiliary chamberlets, the equatorial chamberlets around the embryon and adauxiliary chamberlets isolated and arcuate in shape, cyclic growth attained in neanic stage, the annular chamberlets typically hexagonal, annuli displays wavy pattern.

This species is not yet discriminated into subspecies. *Nemkovella daguini* occurring in 182 m and upwards in the Baskil section was previously illustrated from the coeval beds of the Kırkgeçit Formation in the same area by Özcan et al. (2006; pl. 2, Figs. 1–4). Common in the peri-Mediterranean region, this species was recently reported from the lower Priabonian Tahwah Formation in the Arabian Peninsula and from the transitional middle-upper Eocene Prang Formation in Meghalaya (India) suggesting a wide geographic distribution in the Tethys (Özcan et al. 2019). The upper stratigraphic limit of the species was proposed to extend into SBZ19 by Less and Özcan (2012), although recently Yücel et al. (2019) discovered it from SBZ20 in the Thrace Basin in Turkey.

Orbitoclypeus varians (Kaufmann, 1867)

Orbitoclypeus varians is an unribbed species with "marthae"-type rosette, small- to medium-sized excentri- to eulepidine embryon, adauxiliary chamberlets of "varians" type with moderate size and shape and also moderately wide and high equatorial chamberlets arranged into undulated annuli with "varians"-type growth pattern. This species includes six subspecies in the Tethys: *O. varians portnayae* Less, 1987 ($D_{mean} < 165$ µm); *O. varians* n. ssp. Caupenne ($D_{mean} = 165–205$ µm); *O. varians angoumensis* Less, 1987 ($D_{mean} = 205–255$ µm); *O. varians roberti* (Douvillé, 1922) ($D_{mean} = 255–320$ µm); *O. varians scalaris* (Schlumberger, 1903) ($D_{mean} = 320–400$ µm); *O. varians varians* (Kaufmann, 1867) ($D_{mean} > 400$ µm).

Orbitoclypeus varians is the commonest species in the Baskil section occurring in eight levels (Fig. 11). The species is represented by *O. varians scalaris* in the stratigraphically lowest sample (78) and by *O. varians varians* in the upper samples (182, 198, 269, 279, 314, 375, 385) (Fig. 15e–g). According to Less and Özcan (2012), this species became extinct in the Tethys at Eocene–Oligocene boundary.

Orbitoclypeus zitteli (Checchia-Rispoli, 1908)

Orbitoclypeus zitteli is an average-sized, slightly flattened unribbed species with 'marthae'-type rosettes. The rather large embryon is excentrilepidine (very rarely eulepidine). The adauxiliary chamberlets are of 'varians' type, moderately wide and high. The annuli are almost circular or very slightly undulated; their growth pattern is of the 'varians' type.

This species is very similar to *O. varians* externally and internally. The annuli in *O. varians*, however, display strong undulation and this is used as the primary criterion for their distinction. In Özcan et al. (2006), these forms were described as *O.* aff. *varians*, and since then the species name *O. zitteli* was adopted (Özcan et al. 2010). The species was identified in three levels: samples 182, 276 and 385 (Fig. 15h).

Orbitoclypeus douvillei (Schlumberger, 1903)

Orbitoclypeus douvillei is an unribbed species having "chudeaui"-type rosette, a small to relatively large, eu-, tryblio and excentrilepidine embryon, wide and moderately high, "varians"-type adauxiliary chamberlets and also wide and moderately high equatorial chamberlets arranged into circular annuli with "varians"-type growth pattern. This species includes six subspecies in the Tethys: *O. douvillei douvillei* (Schlumberger, 1903) ($D_{mean} < 200$ µm); *O. douvillei yesilyurtensis* Özcan, 2002 ($D_{mean} = 200–260$ µm); *O. douvillei* n. ssp. Gibret ($D_{mean} = 260–340$ µm); *O. douvillei chudeaui* Less, 1987 ($D_{mean} = 340–425$ µm); *O. douvillei pannonicus* Less, 1987 ($D_{mean} = 425–580$ µm); *O. douvillei malatyaensis* Özcan & Less, 2006 ($D_{mean} > 580$ µm).

This species occurs in four samples, and belongs to *O. douvillei pannonicus* in stratigraphically lowest level (sample 78; Fig. 14e, g) and is represented by *O. douvillei malatyaensis* in samples 182 (Fig. 15f), 202 and 276. The highest occurrence of the species in Baskil section is within SBZ17, consistent with the available data from the Western Tethys.

Orbitoclypeus haynesi (Samanta & Lahiri, 1985)

Orbitoclypeus haynesi is an unribbed species with 'marthae'-type rosette, small eulepidine (rarely excentrilepidine) embryon, adauxiliary chamberlets of 'varians'-type of average size and shape, moderately wide and high equatorial chamberlets arranged into strongly undulated annuli with 'varians'-type growth pattern.

This species, not yet discriminated into subspecies in the Tethys, occurs only in sample 78 (early Bartonian) (Fig. 15a–d). At its type-locality in Kutch (India), it is abundant in the early Bartonian (Özcan et al. 2018). Recorded only in Turkey and Tunisia in the peri-Mediterranean region, *O. haynesi* occurs as the only orbitoclypeid species in the Bartonian of the Indian subcontinent.

Orbitoclypeus n. sp. A

This species is characterized by very large piles (pillars) in the central part of the test, which are fused forming a

Fig. 15 Equatorial sections of *Orbitoclypeus haynesi, O. varians,* and *O. zitteli* from the Baskil section. **a**–**d** *O. haynesi* (Samanta & Lahiri), **a** 78–17, **b** 78–47, **c** 78–50, d 78–46, **e**–**g** *O. varians varians* (Kaufmann), **e** 314b-21, **f** 385b-6, **g** 375b-7, **h** *O. zitteli* (Checchia-Rispoli), 385b-7

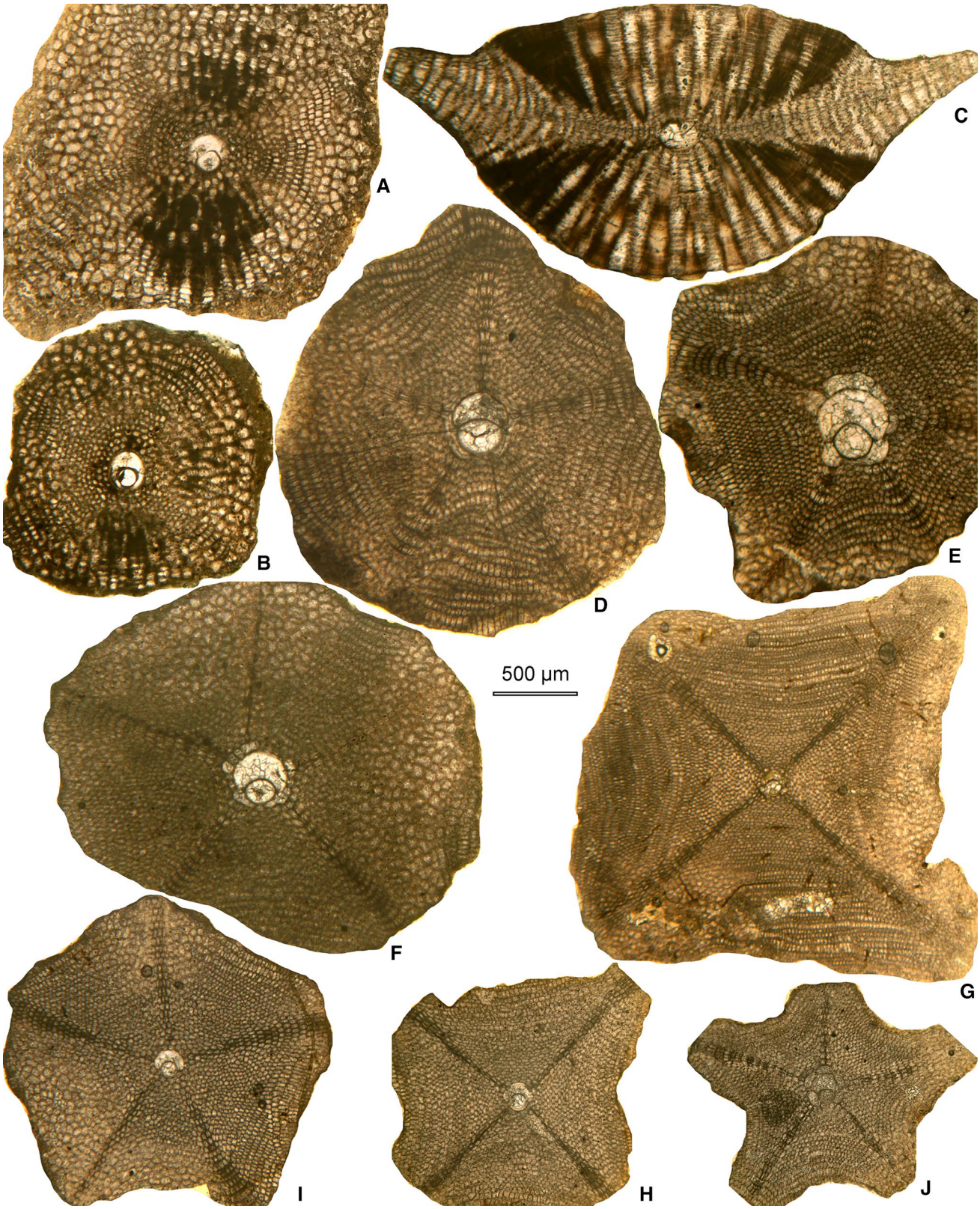

Fig. 16 Equatorial and axial sections of *Orbitoclypeus* n. sp. A and equatorial sections of *Asterocyclina alticostata, A. kecskemetii*, *A. stellata,* and *A. sireli* from the Baskil section. **a**–**c** *Orbitoclypeus* n. sp. A, **a** 182b-29, **b** 182b-27, **c** 182b-66, **d** *A. alticostata* cf. *alticostata* (Nuttall), 279b-6, **e**, **f** *A. kecskemetii* Less, **e** 314b-20, **f** 314b-27, **g**, **h** *A. sireli* Özcan & Less, **g** 78–24, **h** 78–83, **i** *A. stella stella* (Gümbel), 314b-25, **j** *A. stellata stellata* (d'Archiac), 276b-33

thick central pile, covering almost 2/3 of the test surface (Fig. 16c). Internally, the size of protoconch ranges between 110 and 165 µm and that of deuteroconch between 230 and 260 µm. Thus, among the similar taxa, the deuteroconch is much smaller than that of *O. varians* and larger than that of *O. haynesi*. The equatorial chambers are wavy as in *O. haynesi* and *O. varians* (Fig. 16a, b). This species, occurring in samples 182 and 202 in the Bartonian, will be formally described elsewhere.

Asterocyclina sireli Özcan & Less, 2006

Asterocyclina sireli is a medium to large-sized species with four radial ribs and 'marthae'-type rosette. The embryon is small, iso- to nephrolepidine. The deuteroconchal wall corresponding to the position of the successive stage of the developing rib is mostly depressed. The adauxiliary chamberlets are few (2–4) in number, low and moderately wide. The equatorial annuli are arranged usually in four rays.

This species, not yet discriminated into subspecies in Tethys, occurs in three levels: samples 78 (Fig. 16g, h) and 314. Recorded in SBZ16 at its type-locality in Sivas, Turkey (Özcan et al. 2016), its upper range extends into SBZ18. This species, not found in Europe, occurs abundantly in Turkey (Özcan et al. 2006), Tunisia (Ben Ismail-Lattrache et al. 2014) and the Indian subcontinent (Ali et al. 2018; Özcan et al. 2018), all records coming from the upper Lutetian and Bartonian deposits.

Asterocyclina stellata (d'Archiac, 1846)

Asterocyclina stellata is a star-shaped species usually with five rays and "marthae"-type rosette. It has a small semi-iso- to nephrolepidine embryon, few, wide and low, "stellata"-type adauxiliary chamberlets and narrow and low equatorial chamberlets arranged into asteroidal annuli with "strophiolata"-type growth pattern. This species includes four subspecies in the Tethys: *A. stellata adourensis* Less, 1987 ($D_{mean} < 150$ µm); *A. stellata stellata* (d'Archiac, 1846) ($D_{mean} = 150–190$ µm); *A. stellata stellaris* (Rütimeyer, 1850) ($D_{mean} = 190–240$ µm); *A. stellata buekkensis* Less, 1987 ($D_{mean} > 240$ µm).

Asterocyclina stellata in Baskil section belongs to *A. stellata stellata* in samples 78, 182 and 276 (Fig. 16j). It was identified at species level in sample 385.

Asterocyclina stella (Gümbel, 1861)

Asterocyclina stella is a star-shaped species commonly with five rays and "marthae"-type rosette. It has a small semi-iso- to nephrolepidine embryon, few, wide and low, "varians"-type adauxiliary chamberlets and narrow and low equatorial chamberlets arranged into asteroidal annuli with "strophiolata"-type growth pattern. This species includes two subspecies in the Tethys: *A. stella praestella* Less & Kovács, 2009 ($D_{mean} < 150$ µm); *A. stella stella* (Gümbel, 1861) ($D_{mean} > 150$ µm).

Asterocyclina stella in Baskil section belongs to *A. stella stella* in samples 78, 182, 276, 314 (Fig. 16i), 375 and 385.

Asterocyclina alticostata (Nuttall, 1926)

Asterocyclina alticostata is a star-shaped species with five to ten ribs and "chudeaui"-type rosette. It has a medium-sized to relatively large isolepidine embryon, very few, very wide and moderately low, "alticostata"-type adauxiliary chamberlets and also wide and moderately high equatorial chamberlets arranged into asteroidal annuli with "strophiolata" or "varians"-type growth pattern. This species includes four subspecies in the Tethys; *A. alticostata gallica* Less, 1987 ($D_{mean} < 275$ µm); *A. alticostata cuvillieri* (Neumann, 1958) ($D_{mean} = 275–350$ µm); *A. alticostata alticostata* (Nuttall, 1926) ($D_{mean} = 350–450$ µm); *A. alticostata danubica* Less, 1987 ($D_{mean} > 450$ µm).

This species occurs in four levels and was assigned to *A. alticostata cuvillieri* in sample 78 and to *A. alticostata* cf. *alticostata* in samples 182, 279 (Fig. 16d) and 314. According to Less and Özcan (2012), this species become extinct at SBZ19A-B boundary within the Priabonian. Our recent data from Thrace Basin in Turkey, however, show that this species occurs in SBZ20 suggesting that it survived in the latest Priabonian (Yücel et al. 2019).

Asterocyclina kecskemetii Less, 1987

Asterocyclina kecskemetii is a star-shaped form with five to six rays and "chudeaui"-type rosette. It has a medium-sized nephro- to semi-isolepidine embryon, with relatively wide and high, "varians"-type adauxiliary chamberlets. The two principal auxiliary chamberlets are characteristically well developed. The equatorial chamberlets are of average width and height, arranged into sharp asteroidal annuli while their growth pattern is of "strophiolata" type.

This species, not yet subdivided into subspecies in the Tethys, occurs in three levels; samples 182, 276 and 314 (Fig. 16e, f). According to Less and Özcan (2012), this species became extinct at the SBZ19–20 boundary.

Nummulitids

For the generic classification of the family, we apply Hottinger (1977) principles and subdivision with the addition by Romero et al. (1999) on the distinction of *Assilina* and *Operculina*. Four genera are recorded, three of them (*Nummulites*, *Assilina* and *Operculina*) with unsubdivided chambers, and *Heterostegina* with subdivided chambers.

According to Hottinger (1977) and Schaub (1981), the taxonomical concept of nummulitids with no secondary chamberlets is typological and we mostly followed this practice in the determinations. Simultaneously, we apply the morphometric method, used for the orthophragmines, to *Heterostegina* (Less et al. 2008) and to the *Nummulites fabianii*-lineage (Özcan et al. 2009, 2010). Biometric calibration of some other nummulitid lineages is also in progress, and preliminary results (Less 1998b and unpublished data) are used particularly for the *N. perforatus*- and *A. schwageri-alpina*-lineages.

Brief information on the identified taxa is given below, "P" indicates the inner cross-diameter of the proloculus of megalospheric forms.

Genus *Nummulites* Lamarck, 1801 The determination of *Nummulites* is based on both the surface characteristics and the features of the equatorial section. Based on their surface characteristics, the representatives of the genus *Nummulites* in the studied area can be classified into three categories as follows: *N. garganicus*, *N. hormoensis* and *N. ptukhiani* belong to the reticulate, *N. perforatus–biedai* and *N. gizehensis–lyelli* to the granulate, while *N. maximus*, *N. striatus*, *N. biarritzensis* and *N. anomalus* to the radiate forms. Among these taxa, the diameter of microspheric forms of *N. perforatus–biedai*, *N. gizehensis–lyelli* and *N. maximus* exceeds at least 1.5 cm, they are called giant *Nummulites*. Their proloculus size is also large, around 1 mm.

Among the reticulate forms *N. ptukhiani* with relatively large proloculus considerably differs (Cotton et al. 2015) from *N. garganicus* and *N. hormoensis*, which belong to the *N. fabianii*-lineage with much smaller proloculus. Numerous populations of this lineage from the Western Tethys, spanning from the early Bartonian to the early Chattian, are elaborated and the lineage is revised according to the measurement and parameter system introduced by Drooger et al. (1971) and Less (1999). According to Özcan et al. (2009, 2010), the lineage is subdivided into six species, among which *N. garganicus* is characterized by P_{mean} = 100–140 µm, whereas this parameter is between 140 and 200 µm for *N. hormoensis*.

Among giant *Nummulites,* the size increase of the proloculus by time is well documented by Schaub (1981), Serra-Kiel (1984) and Less (1998b). A biometric calibration for the Middle Eocene representatives of this group is in progress, the preliminary results are used in this work.

According to Schaub (1981), radiate *Nummulites* listed above belong to different lineages distinguishable using Schaub's typological criteria. The developmental stage within these lineages was also determined by the Schaub (1981) and by the measurements listed in Less (1998b) too.

***Nummulites garganicus* Tellini, 1890 (Fig. 17a–e)**

This small reticulate taxon (represented exclusively by A-forms) belongs to the *Nummulites fabianii*-lineage, preceded by *N. bullatus* and followed by *N. hormoensis*, from which it is bounded by the arbitrary morphometric limits of P_{mean} = 100 and 140 µm, respectively. More information on the lineage and its segmentation can be found in Özcan et al. (2009, 2010) and in Less et al. (2011, 2018). *N. garganicus* can be commonly found in the lower part of the Baskil section starting from sample 182 up to sample 279; however, higher up it is substituted by *N. hormoensis* (see there). P_{mean} varies between 97 and 120 µm and also fluctuates between samples 182 and 276 (Fig. 18). In strict sense, the population from sample 186.5 is transitional between *N. bullatus* and *N. garganicus*. This population is, however, arranged also here because both the under- and overlying populations surely belong to *N. garganicus*. This taxon was also mentioned from the corresponding sample KEÇ 1 of the nearby Keçili section by Özcan et al. (2006, Table 3 and Pl. 1, Fig. 4, and erroneously under the name of *N.* n. sp. aff. *ptukhiani* on text—Fig. 8). *N. garganicus* characterizes the SBZ17 Zone in most cases, the only exception where it could be found in SBZ18B is recorded by Less et al. (2011).

***Nummulites hormoensis* Nuttall & Brighton, 1931 (Fig. 17f–h)**

This taxon represents the next evolutionary step of the *Nummulites fabianii*-lineage after *N. garganicus*. P_{mean} = 140 µm is the morphometrical limit, which arbitrarily bounds them, while P_{mean} = 200 µm separates it from the successive *N. fabianii*. *N. hormoensis* (only megalospheric specimens) is common in the upper part of the Baskil section starting from sample 314 up to sample 385. As seen in Fig. 18, P_{mean} fluctuates around 150–160 µm in this interval, which, however, differs considerably from the P_{mean} values of *N. garganicus* from the stratigraphically lower samples. *N. hormoensis* was also mentioned from the corresponding sample KEÇ 3 (and also from the stratigraphically higher samples KEÇ 11 and 15) of the nearby Keçili section by Özcan et al. (2006, Table 3 and Pl. 1, Figs. 9 and 17, and erroneously under the name of *N. ptukhiani* on text—Fig. 8). This taxon characterizes the SBZ18 Zone, and in this work we report for the first time the almost synchronous first appearance of *N. hormoensis* with that of the genera *Heterostegina*, *Chapmanina* and *Silvestriella*, above the last occurrence of *N. ptukhiani*, *Assilina exponens*, *Discocyclina pulcra* and *Orbitoclypeus douvillei*.

***Nummulites ptukhiani* Z.D. Kacharava, 1969 (Fig. 19g, h)**

Megalospheric specimens of this reticulate taxon with large (450–1200 µm) proloculus can commonly be found in the middle part of the Baskil section between samples 199 and

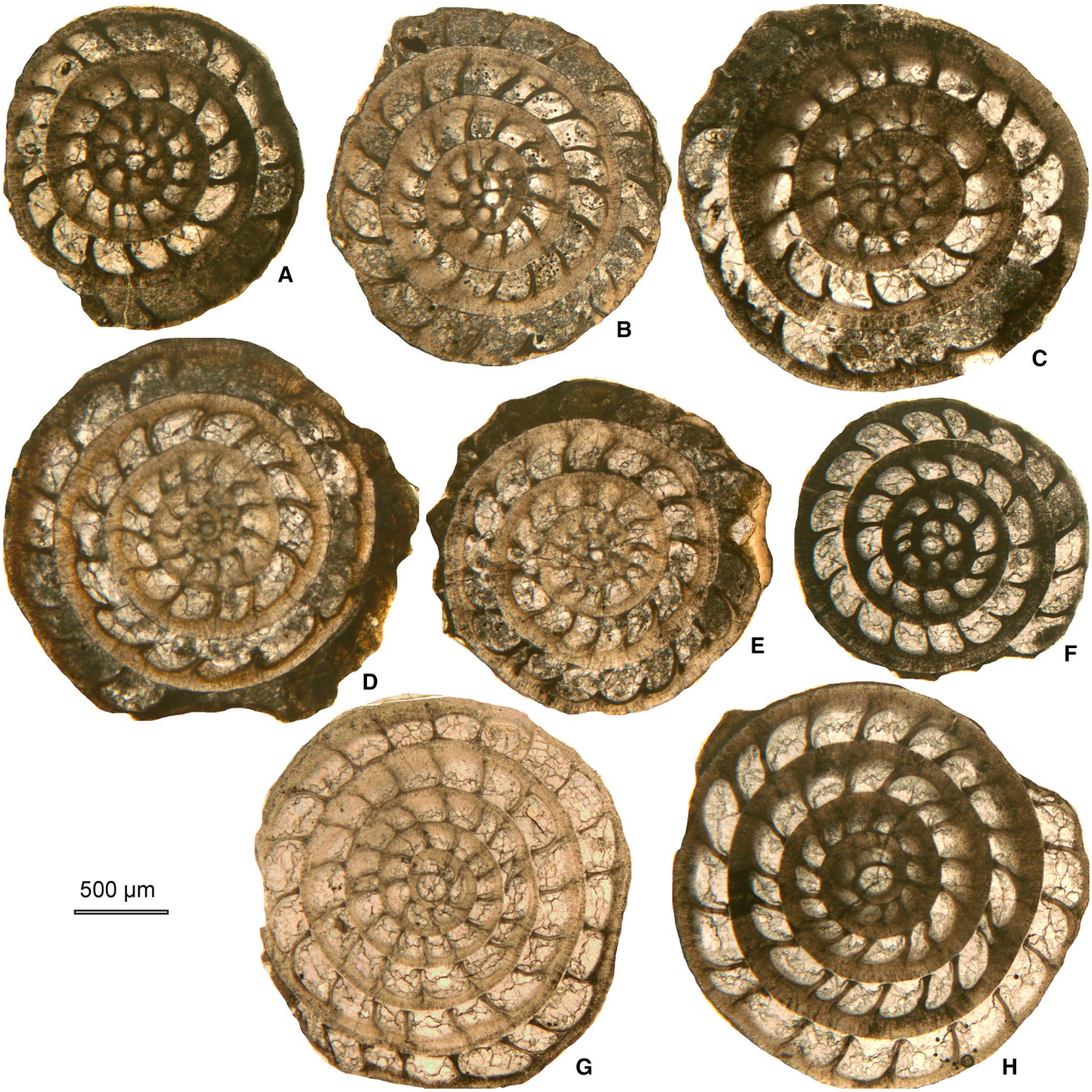

Fig. 17 Equatorial sections of *Nummulites garganicus* and *N. hormoensis* from the Baskil section. **a**–**e** *N. garganicus* Tellini, **a** 182b-2, **b** 182b-9, **c** 182b-1, **d** 202b-1, **e** 202b-2, **f**–**h** *N. hormoensis* Nuttall & Brighton, **f** 314b-1, **g** 385b-1, **h** 314b-3

279 (with no apparent trend in change of the proloculus size); however, it is absent from the stratigraphically higher samples. Özcan et al. (2006) reported this form from the corresponding sample KEÇ 1 of the nearby Keçili section under the name of *N. hottingeri*. This can be explained that *N. ptukhiani* was formerly used (e.g., by Schaub, 1981 and Serra-Kiel et al. 1998) to identify the precursor form of *N. fabianii* (what is called in this work as *N. hormoensis*). However, the original *N. ptukhiani* introduced by Z.D. Kacharava (1969) does not belong to the *N. fabianii*-lineage (for details see Papazzoni, 1998 and Cotton et al. 2015) but corresponds clearly to Schaub's (1981) *N. hottingeri* introduced for reticulate forms with much larger proloculus from the Bartonian. Thus, *N. ptukhiani* is a senior synonym of *N. hottingeri* and should be used instead of it. Cotton et al. (2015) reported the Lutetian precursors of this taxon from Tanzania. However, it became widespread in the Tethys only in the early Bartonian SBZ17, since it is reported from Spain through Turkey

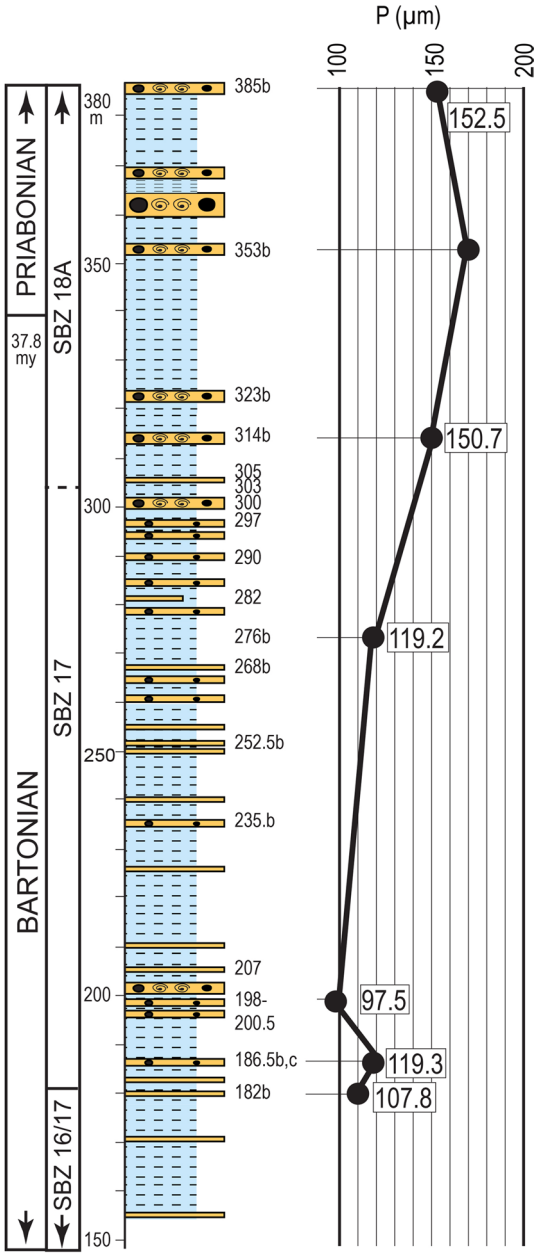

Fig. 18 Change in the inner cross-diameter of the proloculus (p) of reticulate *Nummulites* in the Baskil section

and Armenia to Tanzania and Kutch (Saraswati et al. 2017, who—in our opinion—described the same forms also as *N.* aff. *hormoensis*). *N. ptukhiani* became extinct most probably at the SBZ17/18 boundary since no record of the taxon is known from SBZ18.

Nummulites perforatus (de Montfort, 1808)–*biedai* Schaub, 1962 (Fig. 19c–e)

Advanced representatives of the *Nummulites perforatus*-group are widespread throughout the Baskil section. The sexual dimorphism of this group is quite remarkable. The diameter of inflate, densely granulated B-forms is 1.5–2 cm, whereas that of the A-forms with similar external characteristics is commonly 3–5 mm. Schaub (1981) typologically distinguished more than 20 middle Eocene species of this group, and arranged them into 6 lineages. We hypothesize that several characteristics used for the separation of these taxa are ecophenotypical features because this meticulous taxonomical segregation has not yet been followed in the subsequent works.

The most important numerical feature given by Schaub (1981) for the *N. perforatus*-group is "P", increasing from about 500 µm in the early Lutetian to more than 1000 µm at the top Bartonian. Based on the measurements of all megalospheric specimens of the Schaub-collection in Basel, Less (1998b) confirmed this trend. In collaboration with Dr. Botond Kertész (Budapest, Hungary), we also morphometrically investigated the A-forms of the *N. perforatus*-group from several middle Eocene localities throughout the Western Tethys. Based on our preliminary results (partly published in Özcan et al. 2006, 2010 and Less et al. 2011), upper Lutetian to uppermost Bartonian (and also basal Priabonian according to the most recent interpretation of the Bartonian/Priabonian boundary) representatives of the *N. perforatus*-group are characterized by an average "P" above 700 µm, and (considering also "L", the average length of chambers in the third whorl, introduced by Less, can be arranged into four species. These are: *N. perforatus* with P_{mean} = 700–950 µm and L_{mean} < 420 µm (SBZ16–17), *N. aturicus* with P_{mean} = 700–950 µm and L_{mean} = 420–600 µm (SBZ15–18A), *N. meneghinii* with P_{mean} = 700–950 µm and L_{mean} > 600 µm (SBZ16–17) and *N. biedai* with P_{mean} > 950 µm (SBZ18).

No detailed morphometrical studies were performed in the Baskil section, only "P" was measured and "L" was estimated on some specimens. Based on these, "P" is around 950 µm throughout the section with no significant trend from the base to the top, whereas chambers in the third whorl are relatively narrow, and "L" is commonly smaller than 400 µm. Therefore, we determined the representatives of the *N. perforatus*-group throughout the Baskil section as intermediate between *N. perforatus* and *N. biedai*. It is worth mentioning that formerly a detailed morphometrical study of the group was performed in sample KEÇ 1 from the closest vicinity (Özcan et al. 2006), corresponding to the interval between samples 199b and 276b of the Baskil section, and that population was determined as *N. perforatus*.

Nummulites maximus d'Archiac, 1850 (Fig. 19f, l)

This other giant *Nummulites* in the Baskil section belongs to the *N. millecaput*-group, and is less common than the representatives of the *N. perforatus*-group. They occur in large

quantity only in samples 78 and 276, whereas in the other samples they can only be subordinately found. Giant (up to 5 cm in diameter), flat B-forms occur sporadically. A-forms can be recognized based on the lack of surface granulation and on the characteristic, rather densely spaced, strongly arched septa. "P" is ca. 1000 µm throughout the whole section, and based on this they are considered as *Nummulites maximus*, the most developed member of the *N. millecaput*-group. In the nearby Keçili section, these forms were also found (Özcan et al. 2006) but only in the lowest samples (KEÇ 1 and 3), corresponding to the middle and upper part of the Baskil section. The nomenclatural problems of this group are detailed in Less et al. (2011). Similar forms in slightly higher stratigraphical position (certainly within the SBZ18C Zone, whereas the very rare occurrence of A-forms only in the SBZ19A Zone) were found in the Urtsadzor section of Armenia by Cotton et al. (2017) from where they are reported as *N. millecaput*-group.

Nummulites gizehensis Forskål, 1775–*lyelli* d'Archiac & Haime, 1853 (Fig. 19a, b)

One single juvenile microspheric specimen of this giant *Nummulites* was found in sample 202, unequivocally recognized based on its characteristic surface and almost straight septa; however, determination on the species level was not possible. The characteristic spiral multiplication is well visible in Fig. 19a (for details see Ferràndez-Cañadell 2012). In the nearby Keçili section, Özcan et al. (2006) reported *N. gizehensis* from sample KEÇ 3 corresponding to the highest part of the Baskil section, and also *N. lyelli* from the even higher sample KEÇ 11. This latter species was also found in both the southern (Özcan et al. 2010) and northern (Less et al. 2011) part of the Thrace Basin in basically the same stratigraphic level as in Keçili.

Nummulites striatus (Bruguière, 1792) (Fig. 19m–p)

Both A- and B-forms of this taxon commonly occur throughout the Baskil section except in sample 78, the lowest one containing LBF. Based on the characteristic surface, on the tight spire and also on the densely spaced, moderately arched chambers, it can confidently be identified with *Nummulites striatus*, although Özcan et al. (2006) determined them as *N. cyrenaicus* and *N.* aff. *cyrenaicus* from the nearby Keçili section. No marked trend in parameter "P" (varying between 180 and 360 µm) along the section can be observed. According to Schaub (1981) and Serra-Kiel et al. (1998), this taxon is characteristic for the SBZ18 and also for the SBZ19A Zones. However, in the Baskil section, it starts to occur already from sample 186.5, thus it can also be found in the SBZ17 Zone. Meanwhile, we have never found it above the SBZ18 Zone, and, therefore, we think that the occurrences of *N. striatus* (and also of *N. boulangeri*) from the SBZ19A Zone (e.g., Faudon, Arguis, Villa Marbella) listed by Schaub (1981) should be revised.

Nummulites biarritzensis d'Archiac in Bellardi, 1852 (Fig. 19j, k)

This radiate taxon occurs quite commonly in the Baskil section and it is quite frequent in samples 266 and 276. It bears a relatively small embryon, evenly coiled spiral and slightly arched, more or less isometric chambers. Parameter "P" varies mostly between 100 and 200 µm, with no real trend throughout the section. Özcan et al. (2006) described similar forms from the nearby Keçili section under the name of *Nummulites incrassatus*. Those forms are mostly from slightly younger levels (samples KEÇ 3–16) and possess a slightly larger proloculus (between 140 and 250 µm). Less et al. (2011) also described similar forms from both the SBZ18 and 19 Zones of N Thrace (Turkey) as *N. incrassatus*. Parameter "P" of forms from the SBZ19 Zone is only slightly larger than that from the SBZ18 Zone. Thus, the separation of *N. biarritzensis* and *N. incrassatus* is problematic and not yet solved. However, the former name has priority (de la Harpe, 1883). If further studies demonstrate a real difference between the two species, they can be arranged into a lineage starting with *N. biarritzensis* (?SBZ17–18), followed by *N. incrassatus* (?SBZ19–20) and finishing with *N. vascus* in the Oligocene. The connection between the last two species (although their separation is not yet morphometrically defined, too) was already recognized by Boussac (1911) and followed by several authors as summarized in Nemkov (1967). This is not mentioned by Schaub (1981), although he supposed a probable link of *N. biarritzensis* with *N. vascus*.

Nummulites anomalus de la Harpe, 1877 (Fig. 19i)

This radiate taxon is easily recognized based on its quite regular, relatively tight spire and especially on the sparsely spaced, extremely arched septa. A-forms occur in large numbers only in sample 78 representing SBZ16/17, however, they can also be found sporadically in the higher levels of the Baskil section (samples 279 and 358, representing SBZ17 and 18A, respectively). Microspheric forms were not found. Parameter "P" varies between 140 and 210 µm. Similar forms were also found in the nearby Keçili section (Özcan et al. 2006) in samples KEÇ 3, 11, 15 and 16 (SBZ18A for the first and SBZ18B for the rest) as well as in sample V1.25 of the Urtsadzor section in Armenia (Cotton et al. 2017), corresponding to the SBZ18C Zone. A similar form (but with much smaller proloculus), *Nummulites stellatus* is believed to be characteristic for the SBZ19–20 Zones; however, recently it was also reported from the

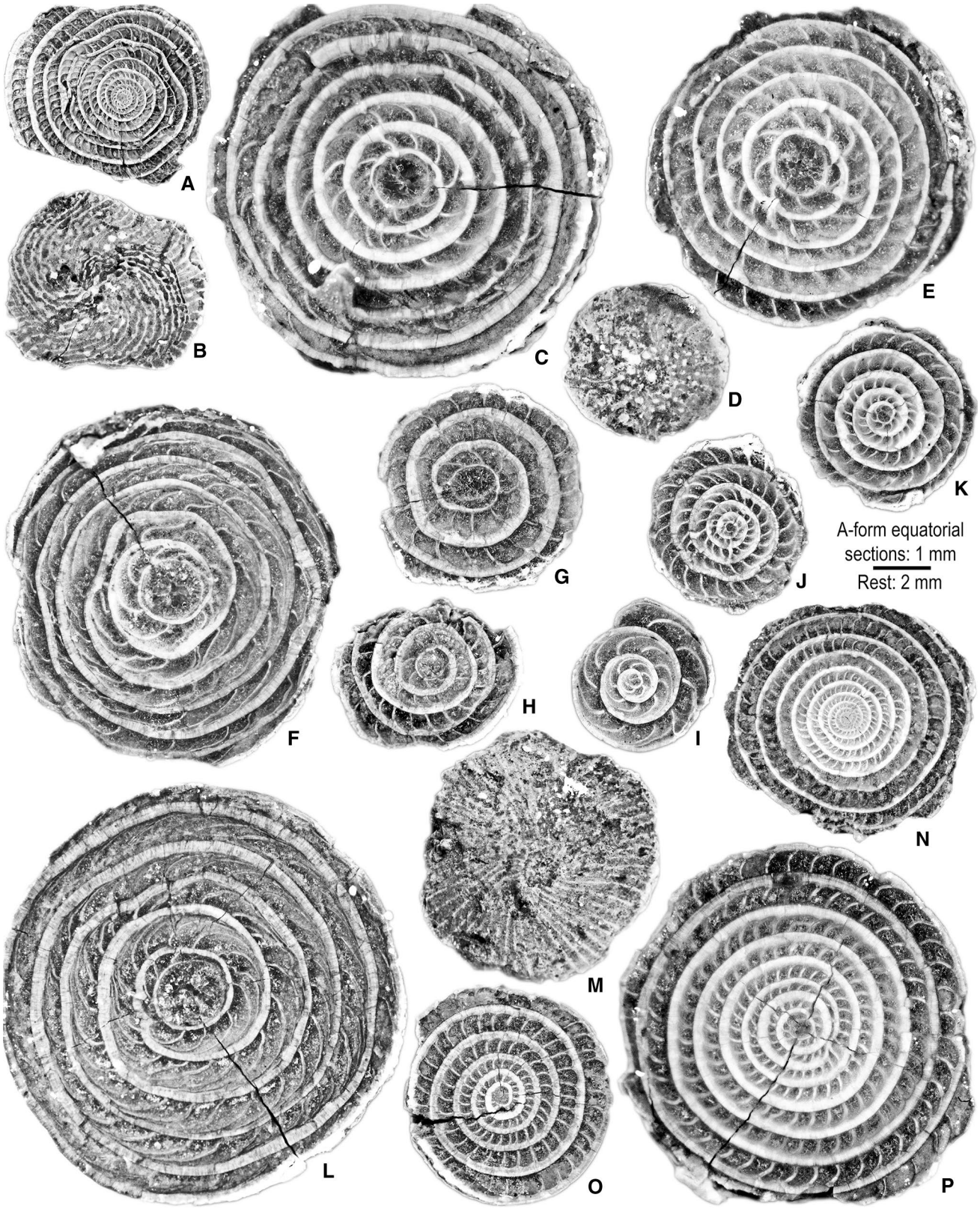

SBZ18B Zone of northern Thrace Basin (Less et al. 2011). Otherwise, *N. anomalus* is very rarely reported, particularly

◂**Fig. 19** Some important *Nummulites* species from the Baskil section. **a**, **b** *Nummulites* ex gr. *gizehensis* (Forskål)–*lyelli* d'Archiac & Haime juvenile specimen, 186-5b, E 2019.1.1. **c**–**e** *Nummulites perforatus* (Montfort), **c** 276b, E 2019.2.1; **d**, **e** 186-5b, E 2019.3.1. **f**, **l** *Nummulites maximus* d'Archiac, **f** 78b, E 2019.4.1; **l** 276b, E 2019.5.1. **g**, **h** *Nummulites ptukhiani* Z. Kacharava, **g** 276b, E 2019.6.1; **h** 242b, E 2019.7.1. **i** *Nummulites anomalus* de la Harpe, 78b, E 2019.8.1. **j**, **k** *Nummulites biarritzensis* d'Archiac, **j** 266b, E 2019.9.1; **k** 276b, E 2019.10.1. **m**–**p** *Nummulites striatus* (Bruguière), **m**, **n** 186-5b, E 2019.11.1; **o** 314b, E 2019.12.1; **p** 266b, E 2019.13.1. **a**, **b**, **m**, **n** B-forms, rest: A-forms. **b**, **d**, **m** External views, rest: equatorial sections. **a**, **b**, **d**, **m**, **n** ×5, rest: ×10

in the last 50 years, and a modern taxonomic revision is required. Therefore, our taxonomic identification is somewhat tentative.

Genus *Assilina* d'Orbigny, 1839 Representatives of this genus belong to two groups. The first of them (*Assilina* in traditional sense) is formed by the large-sized, semi-involute forms of the early and middle Eocene that are arranged by Schaub (1981) into the main *A. spira*- and *A. exponens*-lineages and into the side-lineage of *A. reicheli*. Based on Romero et al. (1999), the small evolute forms ranging through the whole Eocene, formerly generally referred to as *Operculina alpina*, *O. schwageri*, etc., also belong to the genus *Assilina*.

***Assilina exponens* (Sowerby, 1840)**

Megalospheric forms of this taxon occur constantly in the lower and middle part of the Baskil section (up to sample 276), and they were also reported from the corresponding sample KEÇ 1 of the nearby Keçili section (Özcan et al. 2006). Unfortunately, we failed to obtain good equatorial sections; however, we could measure parameter "P" (350–550 µm). The specific determination of large *Assilina* (Schaub, 1981) is purely based on typological features. In the case of the Baskil material, we used also the fact that *A. exponens* was first described from the Fulra Limestone of Lakhpat (Kutch, W India) having according to Özcan et al. (2018) and Saraswati et al. (2018) the same age (SBZ17) as the Baskil samples containing *Assilina*. Since large-sized semi-involute *Assilina* specimens have never been reported from stratigraphically higher levels, their highest occurrence marks reliably the SBZ17/18 zone boundary together with the highest or lowest occurrence of some other forms listed at the end of the description of *N. hormoensis*.

***Assilina schwageri* (Silvestri, 1928) (Fig. 20f, g)**

Based on Romero et al. (1999) the evolute forms, formerly referred to as *Operculina alpina*, *O. schwageri*, etc., belong to the genus *Assilina*, since their septa are not folded and not intersected by stolons characteristic for *Operculina*. According to Hottinger (1977), this group forms a single evolutionary lineage. It needs, however, a serious revision since biometric limits between chronotaxa are not yet established. However, basing on the data of Papazzoni (1998), Less (1999), Özcan et al. (2010) and Less et al. (2011), it can be recognized that for forms from the SBZ17–18 Zones "P" below 120 µm is characteristic whereas for those from the SBZ19–20 Zones this value is commonly above 120 µm.

In the entire Baskil section, megalospheric specimens of these evolute *Assilina* occur constantly as accessorial elements of the LBF fauna as well as in the nearby Keçili section (Özcan et al. 2006 where they were determined as *Assilina* ex. gr. *schwageri–alpina*), and "P" is mostly between 60 and 135 µm with no stratigraphically increasing trend. Since traditionally the forms from older levels are called *A. schwageri* whereas the name of *A. alpina* is used for those from the younger strata, we tentatively apply the name of *A. schwageri* for specimens from both the Baskil and Keçili sections.

Genus *Operculina* d'Orbigny, 1826 This genus with folded septa intersected by stolons is represented in the Eocene by the involute *Operculina gomezi*-group with very dense and high chambers.

***Operculina* ex gr. *gomezi* Colom & Bauzá, 1950 (Fig. 20d, e)**

The first appearance of the *Operculina gomezi*-group nearly coincides with the Lutetian/Bartonian boundary (see Özcan et al. 2006; Less and Özcan 2012). In the Baskil section, A-forms of this group were first recognized in sample 186.5, and then, starting from sample 276b they constantly occur up to the top of the profile, as well as in the neighboring Keçili section (Özcan et al. 2006, under the name *O.* ex gr. *roselli–gomezi*). Hottinger (1977) arranged the representatives of the *O. gomezi*-group into a single evolutionary lineage starting with *O. bericensis*, followed by *O. roselli* and ending with *O. gomezi*; however, their biometric limits have not been given. Therefore, here we apply the name of *O.* ex gr. *gomezi*. In our material, the inner cross-diameter of the proloculus does not show a clear increasing trend and remains in the range between 80 and 130 µm.

Genus *Heterostegina* d'Orbigny, 1826 Based on a rather wide Mediterranean material the Eocene representatives of this genus have been revised by Less et al. (2008), who arranged them into three lineages considered as species. These are *H. armenica*, *H. reticulata* and *H. gracilis*; among which only the first of them occurs in the Baskil section.

***Heterostegina armenica armenica* (Grigoryan, 1986) (Fig. 20a–c)**

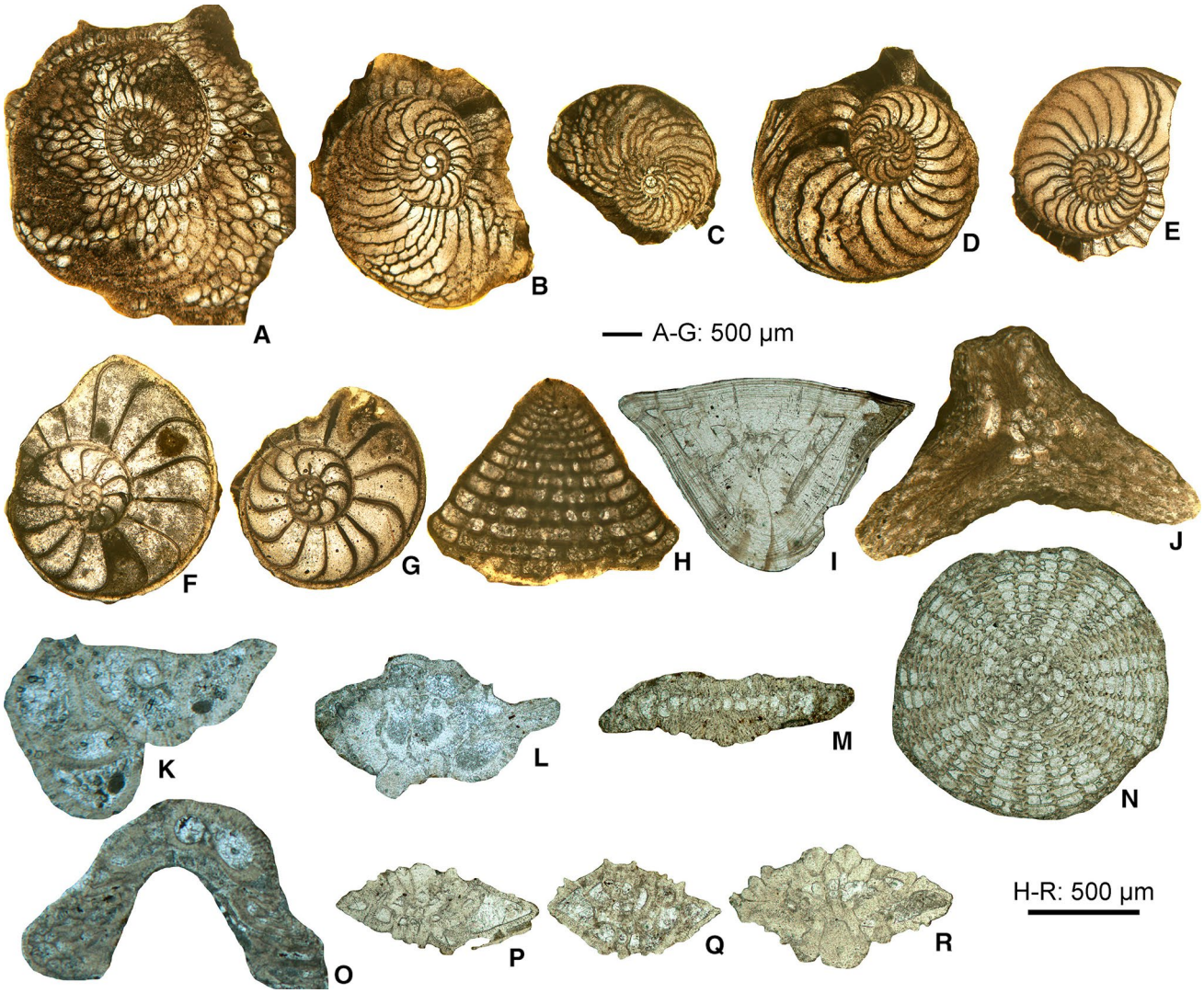

Fig. 20 Stratigraphically important nummulitids from the Baskil section. **a**–**c** Heterostegina armenica armenica (Grigoryan), **a** 385b-16, **b** 375b-4, **c** 375b-3, **d**, **e** Operculina ex gr. gomezi Colom & Bauzá, **d** 375b-1, **e** 314b-16, **f**, **g** Assilina schwageri (Silvestri), **f** 385b-19, **g** 314b-17, **h** Chapmanina gassinensis (Silvestri), 375b-14, **i** Asterigerina rotula (Kaufmann), 197, **j** Silvestriella tetraedra (Gümbel), 375b-15, **k** Gyroidinella sp. 353, **l** Calcarina sp., 297, **m** Linderina sp. 197, **n** Sphaerogypsina globulus (Reuss), 201, **o** Fabiania cassis (Oppenheim), 353, **p**–**r** rotaliid foraminifer, 186.5

The representatives of the *H. armenica*-lineage have an involute, flat biconvex test, a central pile and slightly sigmoid septal sutures passing into an irregular sutural network in the edges. The proloculus is relatively large (as compared with the representatives of the *H. reticulata* lineage with similar *X* values; see later), the chamberlets (often with incomplete secondary septa) are rather irregularly arranged and characteristically polygonal. The number of undivided chambers is subjected to nepionic acceleration. Based on this, the species has been subdivided by Less et al. (2008, 2011) into three chronosubspecies as follows (parameter *X* marks the number of post-embryonic, pre-heterosteginid chambers): *H. armenica armenica* ($X_{mean} > 8$), *H. armenica tigrisensis* ($X_{mean} = 5–8$) and *H. armenica hacimasliensis* ($X_{mean} < 5$). According to Less et al. (2008), *H. armenica armenica* is characteristic for the SBZ18A, while the other two, more advanced subspecies for the SBZ18B Subzone.

In the Baskil section, megalospheric forms of the lineage are absent in the lower and middle part, they first appear only in sample 323b, and upsection they occur also in samples 375b and 385b. In the Keçili section, they are also missing from the lowest sample KEÇ 1 but are present upsection in samples KEÇ 3 (corresponding to the upper part of the Baskil section), and further in samples KEÇ 11, 15 and 16. Based on the above diagnosis, Less et al. (2008) identified the population from sample KEÇ 3 as *H. armenica armenica*, and those from the other samples as *H. armenica tigrisensis*. Since the developmental degree of specimens from

the upper part of the Baskil section is very similar to that from sample KEÇ 3, these populations are also identified as *H. armenica armenica*.

Chapmanina, *Silvestriella*, *Linderina* and *Calcarina*

The genera *Linderina* (Fig. 20m) and *Calcarina* (Fig. 20l) occur rarely in the Bartonian part of the Baskil section (Fig. 4). *Chapmanina*, represented by *C. gassinensis* (Silvestri) (Fig. 20h), and *Silvestriella*, represented by *S. tetraedra* (Gümbel) (Fig. 20j) appear first in the lower part of SBZ18A, close to the Bartonian–Priabonian boundary. Thus, the first appearance datum level of these taxa is significant to the tentative placement of the Bartonian–Priabonian boundary. We have also identified the following additional LBFs in the section; *Asterigerina rotula* (Kaufmann) (Fig. 20i), *Gyroidinella* sp. (Figure 20k), *Sphaerogypsina globulus* (Reuss) (Fig. 20n), *Fabiania cassis* (Oppenheim) (Fig. 20o), and some rotaliid foraminifera (Fig. 20p–r).

Conclusions

The Baskil section is an expanded Bartonian-early Priabonian deep-marine sequence consisting of diverse assemblages of platform-derived LBF. The magnetic polarity record previously recognized by Rodelli et al. (2018) subdivides the studied section into 12 magnetozones, with 6 reverse polarity and 6 normal polarity intervals spanning from the upper part of Subchron C19n.1r to the base of Subchron C17n.1n (42.4–37.8 Ma). The section spans the planktonic foraminiferal Zones E10/11 to E14, the calcareous nannofossil zones NP15–NP18, LBF zones SBZ16/17 to SBZ18A, including OZ zones OZ12–OZ14. The Bartonian–Priabonian boundary is placed at NP17/18 boundary by the lowest occurrence of *Chiasmolithus oamaruensis,* which lies within Subchron C17n.1n and Zone SBZ18A. This section yielded the richest LBF assemblages in Bartonian and across the Bartonian–Priabonian boundary in the Tethys, which are correlated to deep-marine fauna and biota. We have identified 21 orthophragminid lineages and 13 nummulitid species as well as some stratigraphically diagnostic other genera, such as *Chapmanina, Silvestriella, Linderina* and *Calcarina*, listed in the Appendix. Most orthophragminid species straddle the Bartonian–Priabonian boundary, while two species, *O. douvillei* and *D. pulcra* appear to be confined to SBZ18 at their upper stratigraphic ranges. The representatives of *Nummulites fabianii*-lineage show a clear increase in embryon diameters and are represented by *N. garganicus* and *N. hormoensis*, respectively. Their transition, together with the first appearance of the genera *Heterostegina, Chapmanina and Silvestriella* and also with the last occurrence of *N. ptukhiani*, *Assilina exponens*, *Discocyclina pulcra* and *Orbitoclypeus douvillei* in the upper part of the section suggest that these are the best LBF markers to tentatively infer to Bartonian–Priabonian boundary in the Tethys.

Acknowledgements The Baskil project was developed within the framework of the CAPES (Coordenação de Aperfeiçoamento de Pessoal de Nível Superior) "Ciências do Mar II" and Marie Curie Actions (FP7-PEOPLEIEF-2008, proposal 236311). L. Jovane, D. Rodelli, E.S. Rego and M. Giorgioni were supported by grants from the Fundação de Amparo a Pesquisa do Estado de São Paulo (FAPESP) 2011/22018-3, 2012/21212-3, 2015/16501-4 and 2012/15995-5, respectively. Thanks are due to Johannes Pignatti (Rome) and to Pratul Kumar Saraswati (Mumbai) for constructive reviews. We thank editor Attila Çiner for his comments and suggestions.

Funding The Baskil project was developed within the framework of the CAPES (Coordenação de Aperfeiçoamento de Pessoal de Nível Superior) "Ciências do Mar II" and Marie Curie Actions (FP7-PEOPLEIEF-2008, proposal 236311).

Compliance with ethical standards

Conflict of interest No potential conflict of interest.

Informed consent Informed consent was obtained from all individual participants included in the study.

Appendix

List of larger benthic foraminifera from the Baskil section.

Discocyclina pratti (Michelin, 1846)
D. trabayensis Neumann, 1955
D. augustae van der Weijden, 1940
D. radians (d'Archiac, 1850)
D. euaensis Whipple, 1932
D. dispansa (Sowerby, 1840)
D. pulcra (Checchia-Rispoli, 1909)
D. discus (Rütimeyer, 1850)
Nemkovella evae Less, 1987
N. strophiolata (Gümbel, 1870)
N. daguini (Neumann, 1958)
Orbitoclypeus douvillei (Schlumberger, 1903)
O. haynesi (Samanta & Lahiri, 1985)
O. varians (Kaufmann, 1867)
O. zitteli (Checchia-Rispoli, 1908)
Orbitoclypeus n. sp. A
Asterocyclina stellata (d'Archiac, 1846)
A. stella (Gümbel, 1861)
A. sireli Özcan & Less, 2006
A. kecskemetii Less, 1987
A. alticostata (Nuttall, 1926)
Nummulites garganicus Tellini, 1890
N. hormoensis Nuttall & Brighton, 1931
N. perforatus (de Montfort, 1808)–*biedai* Schaub, 1962
N. maximus d'Archiac, 1850

N. gizehensis Forskål, 1775–*lyelli* d'Archiac & Haime, 1853
N. ptukhiani Z.D. Kacharava, 1969
N. striatus (Bruguière, 1792)
N. biarritzensis d'Archiac & Haime, 1853
N. anomalus de la Harpe, 1877
Heterostegina armenica (Grigoryan, 1986)
Operculina ex. gr. *gomezi* Colom & Bauzá, 1950
Assilina schwageri (Silvestri, 1928)
A. exponens (Sowerby, 1840)
Chapmanina gassinensis (Silvestri, 1905)
Silvestriella tetraedra (Gümbel, 1868)
Calcarina sp.
Linderina sp.

References

Agnini C, Fornaciari E, Giusberti L, Grandesso P, Lanci L, Luciani V, Muttoni G, Pälike H, Rio D, Spofforth DJA, Stefani C (2011) Integrated biomagnetostratigraphy of the Alano section (NE Italy): a proposal for defining the middle-late Eocene boundary. Geol Soc Am Bull 123:841–872

Agnini C, Fornaciari E, Raffi I, Catanzariti R, Pälike H, Backman J, Rio D (2014) Biozonation and biochronology of Paleogene calcareous nannofossils from low and middle latitudes. Newsl Stratigr 47:131–181

Akbaş B, Akdeniz N, Aksay A, Altun İ, Balcı V, Bilginer E, Bilgiç T, Duru M, Ercan T, Gedik İ, Günay Y, Güven İH, Hakyemez HY, Konak N, Papak İ, Pehlivan Ş, Sevin M, Şenel M, Tarhan N, Turhan N, Türkecan A, Ulu Ü, Uğuz MF, Yurtsever A (2011) Geological map of Turkey. General Directorate of Mineral Research and Exploration, Ankara

Aksoy E, Türkmen İ, Turan M (2005) Tectonics and sedimentation in convergent margin basins: an example from the Paleogene Elazığ basin, Eastern Turkey. J Asian Earth Sci 25:459–472

Aktaş G, Robertson AHF (1984) The Maden Complex, SE Turkey: evolution of a Neo-Tethyan active margin. In: Dixon JE, Robertson AHF (eds) The geological evolution of the Eastern Mediterranean. Blackwell Scientific Publications, Oxford, pp 375–402

Ali N, Özcan E, Yücel AO, Hanif M, Hashmi SI, Ullah F, Rizwan M, Pignatti J (2018) Bartonian orthophragminids with new endemic species from the Pirkoh and Drazinda formations in the Sulaiman Range, Indus Basin, Pakistan. Geodin Acta 30:31–62

Avşar N (1991) Elazığ bölgesinde *Nummulites fabianii* (Prever) grubunun (*Nummulites* ex. gr. *fabianii*) varlığı ve ilgili foraminiferler. Bull Miner Res Explor 112:155–160

Avşar N (1996) Inner platform sediments with *Praebullalveolina afyonica* Sirel & Acar around Elazığ region (E. Turkey). Bull Miner Res Explor 118:9–14

Ben İsmail-Lattrache K, Özcan E, Boukhalfa K, Saraswati PK, Soussi M, Jovane L (2014) Early Bartonian orthophragminids (foraminiferida) from Reineche Limestone, north African platform, Tunisia: taxonomy and paleobiogeographic implications. Geodin Acta 26:94–121

Bingöl AF (1984) Geology of the Elazığ area in the Eastern Taurus region. In: Tekeli O, Göncüoğlu C (eds) Geology of the Taurus Belt Proceedings of International Tauride Symposium. Mineral Research and Exploration Institute of Turkey Publications, pp 209–216 **(in Turkish with English abstract)**

Boussac J (1911) Études paléontologiques sur le Nummulitique alpin. Mémoires pour servir à l'explication de la carte géologique détaillée de la France, 440 p. + Atlas

Costa E, Garcés M, López-Blanco M, Serra-Kiel J, Bernaola G, Cabrera L, Beamud E (2013) The Bartonian-Priabonian marine record of the eastern South Pyrenean foreland basin (NE Spain): a new calibration of the larger foraminifers and calcareous nannofossil biozonation. Geol Acta 11:177–193

Cotton LJ, Pearson PN, Renema W (2015) A new lineage of reticulate *Nummulites* from Kilwa District, Tanzania; a place for *Nummulites ptukhiani*? J Syst Paleontol 14:569–579

Cotton LJ, Zakrevskaya EY, van der Boon A, Asatryan G, Hayrapetyan F, Israelyan A, Krijgsman W, Less G, Monechi S, Papazzoni CA, Pearson PN, Razumovskiy A, Renema W, Shcherbinina E, Wade B (2017) Integrated stratigraphy of the Priabonian (upper Eocene) Urtsadzor section, Armenia. Newsl Stratigr 50:269–295

Cronin BT, Hartley AJ, Çelik H, Hurst A, Türkmen İ, Kerey E (2000) Equilibrium profile development in graded deep-water slopes: eocene, Eastern Turkey. J Geol Soc Lond 157:943–955

de la Harpe Ph (1883) Étude des Nummulites de la Suisse et révision des espèces éocènes des genres *Nummulites* et *Assilina*. 3ème et dernière partie. Mémoires de la Soc Paléontol Suisse 10(4):141–180

Drooger CW, Marks P, Papp A (1971) Smaller radiate *Nummulites* of northwestern Europe. Utrecht Micropaleontol Bull 5:137

Ferràndez-Cañadell C (1997) A new, ribbed species of *Nemkovella* 1987 (Discocyclinidae), and discussion on the genus *Actinocyclina* Gümbel, 1870. J Foramin Res 27:175–185

Ferràndez-Cañadell C (2012) Multispiral growth in *Nummulites.* Paleobiological implications. Mar Micropaleontol 96–97:105–122

Fornaciari E, Agnini C, Catanzariti R, Rio D, Bolla EM, Valvasoni E (2010) Mid- Latitude calcareous nannofossil biostratigraphy and biochronology across the middle to late Eocene transition. Stratigraphy 7(4):229–264

Gradstein FM, Ogg JG, Schmitz MD, Ogg GM (2012) The geologic time scale 2012. Elsevier Publication, Amsterdam, pp 85–114

Gy Less (1998a) Zonation of the Mediterranean Upper Paleocene and Eocene by Orthophragminae. Opera Dela Slovenska Akademija Znanosti in Umetnosti (4) 34(2):21–43

Gy Less (1998b) Statistical data of the inner cross protoconch diameter of *Nummulites* and *Assilina* from the Schaub collection. Opera Dela Slovenska Akademija Znanosti in Umetnosti (4) 34(2):183–202

Herece Eİ, Acar Ş (2016) Upper Cretaceous-Tertiary geology-stratigraphy of Pertek and its vicinity (Tunceli, Turkey). Bull Miner Res Explor 153:1–44

Hottinger L (1977) Foraminifères operculiniformes. Mém du Muséum Natl d'Histoire Nat 57:159

Hottinger L (2014) Paleogene larger rotaliid foraminifera from the western and central Neotethys. Springer, New York

Hüsing SK, Zachariasse W-J, Van Hinsbergen DJJ, Krijgsman W, İnceöz M, Harzhauser M, Mandic O, Kroh A (2009) Oligocene-Miocene basin evolution in SE Anatolia, Turkey: constraints on the closure of the eastern Tethys gateway. In: Van Hinsbergen DJJ, Edwards MA, Govers R (eds) Collision and collapse at the Africa–Arabia–Eurasia subduction zone, vol 311. The Geological Society, London, special Publications, pp 107–132

Kacharava ZD (1969) On the phylogenetic sequence of the *Nummulites fabianii* group. Bull Sci Acad Georg SSR 55(2):498–500 **(in Russian with English summary)**

Less Gy (1987) Paleontology and stratigraphy of the European Orthophragminae. Geol Hung Ser Palaeontol 51:1–373

Less Gy (1999) The late Paleogene larger foraminiferal assemblages of the Bükk Mts. (NE Hungary). Rev Esp Micropaleontol 31(3):51–60

Less Gy, Özcan E (2012) Bartonian-Priabonian larger benthic foraminiferal events in the Western Tethys. Austrian J Earth Sci 105(1):129–140

Less Gy, Özcan E, Papazzoni CA, Stockar R (2008) The middle to late Eocene evolution of nummulitid foraminifer *Heterostegina* in the Western Tethys. Acta Palaeontol Pol 53:317–350

Less Gy, Özcan E, Okay AI (2011) Stratigraphy and Larger Foraminifera of the Middle Eocene to Lower Oligocene Shallow-Marine Units in the northern and eastern parts of the Thrace Basin, NW Turkey. Turk J Earth Sci 20(6):793–845

Less Gy, Frijia G, Özcan E, Saraswati PK, Parente M, Kumar P (2018) Nummulitids, lepidocyclinids and Sr-isotope data from the Oligocene of Kutch (western India) with chronostratigraphic and paleobiogeographic evaluations. Geodin Acta 30(1):183–211

Lirer F (2000) A new technique for retrieving calcareous microfossils from lithified lime deposits. Micropaleontology 46:365–369

Luciani V, Papazzoni CA, Fornaciari E, Dallanave E, Giusberti L, Stefani C, Amante E (2016) Correlation between shallow benthic and calcareous plankton zones at the Bartonian-Priabonian transition (Varignano section, northern Italy. Soc Geol Ital 40:1001

Martini E (1971) Standard tertiary and quaternary calcareous nannoplankton zonation. In: Farinacci (eds) Proc. II Plankt. Conf. Roma, 1970, Edizioni Technoscienza, vol 2, pp 739–785

Nemkov GI (1967) Nummulitidy Sovetskogo Soyuza i ikh biostratigraficheskoye znacheniye. Nauka **(in Russian)**

Okada H, Bukry D (1980) Supplementary modification and introduction of code numbers of the low-latitude coccolith biostratigraphic zonation (Bukry 1973, 1975). Mar Micropaleontol 5:321–325

Özcan E, Less G, Báldi-Beke M, Kollányi K, Kertesz B (2006) Biometric analysis of middle and upper Eocene Discocyclinidae and Orbitoclypeidae (Foraminifera) from Turkey and updated orthophragmine Zonation in the Western Tethys. Micropaleontology 52:485–520

Özcan E, Gy Less, Báldi-Beke M, Kollányi K, Acar F (2009) Oligo-Miocene Foraminiferal Record (Miogypsinidae, Lepidocyclinidae and Nummulitidae) from the Western Taurides (SW Turkey): biometry and implications for the regional geology. J Asian Earth Sci 34(6):740–760

Özcan E, Less G, Okay AI, Báldi-Beke M, Kollányi K, Yılmaz İÖ (2010) Stratigraphy and larger foraminifera of the eocene shallow-marine and olistostromal units of the southern part of the Thrace Basin, NW Turkey. Turk J Earth Sci 19:27–77

Özcan E, Saraswati PK, Hanif M, Ali N (2016) Orthophragminids with new axial thickening structures from the Bartonian of the Indian subcontinent. Geol Acta 14(3):261–282

Özcan E, Saraswati PK, Yücel AO, Ali N, Hanif M (2018) Bartonian orthophragminids from the Fulra Limestone (Kutch, W India) and coeval units in Sulaiman Range, Pakistan: a synthesis of shallow benthic zone (SBZ) 17 for the Indian Subcontinent. Geodin Acta 30:137–162

Özcan E, Erbay S, Abbasi AI, Pereira CD, Erkızan LS, Kayğılı S (2019) The first record of *Nemkovella daguini* (Neumann, 1958) from the middle-late Eocene of Oman (Arabian Peninsula) and Meghalaya (Indian Subcontinent) and its significance in Tethyan correlations and paleobiogeography. Riv Ital Paleontol Stratigr 125:13–28

Özkul M (1988) Sedimentological investigations on the Kırkgeçit Formation in the western Elazığ. (Ph.D. Thesis): Fırat University Graduate School of Science and Technology, Elazığ–Turkey, p. 186 **(in Turkish with English abstract)**

Papazzoni CA (1998) Biometric analyses of *Nummulites* "*ptukhiani*" Z.D. Kacharava, 1969 and *Nummulites fabianii* (Prever in Fabiani, 1905). J Foraminifer Res 28(3):161–176

Papazzoni CA, Cosovic V, Briguglio A, Drobne K (2017) Towards a calibrated larger foraminifera biostratigraphic zonation: celebrating 18 years of the application of shallow benthic zones. Palaios 32:1–5

Racey A (1995) Lithostratigraphy and larger foraminiferal (nummulitid) biostratigraphy of the Tertiary of northern Oman. Micropaleontology 41:1–123

Rego ER, Jovane L, Hein JR, Sant'Anna LG, Giorgioni M, Rodelli D, Özcan E (2018) Mineralogical evidence for warm and dry climatic conditions in the Neo-Tethys (eastern Turkey) during the middle Eocene. Palaeogeography, Palaeoclimatology, Palaeoecology 501:45–57

Rodelli D, Jovane L, Özcan E, Giorgioni M, Coccioni R, Frontalini F, Rego ER, Brogi A, Catanzariti R, Less G, Rostami MA (2018) High-resolution integrated magnetostratigraphy of a new middle Eocene section from the Neotethys (Elazığ Basin, eastern Turkey). Geol Soc Am Bull 130:193–207

Romero J, Hottinger L, Caus E (1999) Early appearance of larger foraminifera supposedly characteristic for Late Eocene in the Igualada Basin (NE Spain). Rev Esp de Paleontol 14(1):79–92

Saraswati PK, Anwar D, Lahiri A (2017) Bartonian reticulate *Nummulites* of Kutch. Geodin Acta 29(2):14–23

Saraswati PK, Khanolkar S, Banerjee S (2018) Paleogene stratigraphy of Kutch, India: an update about progress in foraminiferal biostratigraphy. Geodin Acta 30(1):100–118. https://doi.org/10.1080/09853111.2017.1408263

Schaub H (1981) Nummulites et Assilines de la Tethys Paléogène. Taxonomie, phylogénèse et biostratigraphie. Schweizerische Paläontologische Abhandlungen, pp 104–106, 1–236 + Atlas I–II

Serra-Kiel J (1984) Estudi dels Nummulites del grup de *N. perforatus* (Montfort) (Conques aquitana, catalana i balear). Treballs de la Institució Catalana d'Història Natural 11:244

Serra-Kiel J, Hottinger L, Caus E, Drobne K, Ferràndez-Cañadell C, Jauhri AK, Less Gy, Pavlovec R, Pignatti J, Samso JM, Schaub H, Sirel E, Strougo A, Tambareau Y, Tosquella J, Zakrevskaya E (1998) Larger foraminiferal biostratigraphy of the Tethyan Paleocene and Eocene. Bull de la Soc Géologique de Fr 169:281–299

Serra-Kiel J, Mató E, Saula E, Travé A, Ferràndez-Cañadell C, Busquets P, Samsó JM, Tosquella J, Barnolas A, Àlvarez-Pérez G, Franquès J, Romero J (2003) An inventory of the marine and transitional Middle/Upper Eocene deposits of the southeastern Pyrenean Foreland Basin (NE Spain). Geol Acta 1:201–229

Serra-Kiel J, Gallardo-Garcia A, Razin Ph, Robinet J, Roger J, Grelaud C, Leroy S, Robin C (2016) Middle Eocene-early Miocene larger foraminifera from Dhofar (Oman) and Socotro Island (Yemen). Arab J Geosci 9:95p

Turan M (1984) The stratigraphy and tectonics of Baskil-Aydınlar (west of Elazığ, E. Turkey) area. (Ph.D. Thesis): Fırat University Graduate School of Science and Technology, Elazığ **(in Turkish with English abstract)**

Türkmen İ, İnceöz M, Kerey İE (1999) Kırkgeçit Formation (Middle Eocene-Oligocene): an example of tidal flat and stormy shelf complex (NNW of Elazığ). Bull Earth Sci Appl Res Centre Hacet Univ 21:125–142 **(in Turkish with English abstract)**

Türkmen İ, İnceöz M, Aksoy E, Kaya M (2001) New findings on Eocene stratigraphy and paleogeography of Elazığ area. Bull Earth Sci Appl Res Centre Hacet Univ 24:81–95 **(in Turkish with English abstract)**

Wade BS, Pearson PN, Berggren WA, Pälike H (2011) Review and revision of Cenozoic tropical planktonic foraminiferal biostratigraphy and calibration to the geomagnetic polarity and astronomical time scale. Earth Sci Rev 104:111–142

Yazgan E (1984) Geodynamic evolution of the Eastern Taurus region. Geology of the Taurus Belt Proceedings of International Tauride Symposium. Mineral Research and Exploration Institute of Turkey Publications, pp 199–208 **(in Turkish with English abstract)**

Yücel AO, Özcan E, Erbil Ü (2019) Late Priabonian Larger Benthic foraminiferal assemblages at the demise of Soğucak carbonate

platform (the Thrace Basin, NW Turkey): implications for the shallow marine biostratigraphy. Turk J Earth Sci

Zakrevskaya E, Beniamovsky V, Gy Less, Báldi-Beke M (2011) Integrated biostratigraphy of Eocene deposits in the Gubs section (Northern Caucasus) with special attention to the Ypresian/Lutetian boundary and to the Peritethyan-Tethyan correlation. Turk J Earth Sci 20(6):753–792

Affiliations

Ercan Özcan[1] · Gy. Less[2] · L. Jovane[3] · R. Catanzariti[4] · F. Frontalini[5] · R. Coccioni[5] · M. Giorgioni[3,6] · D. Rodelli[3] · E. S. Rego[3,7] · S. Kayğılı[8] · M. Asgharian Rostami[9]

[1] Department of Geological Engineering, Faculty of Mines, İstanbul Technical University (İTÜ), Maslak, 34469 Istanbul, Turkey

[2] Institute of Mineralogy and Geology, University of Miskolc, Miskolc-Egyetemváros 3515, Hungary

[3] Instituto Oceanográfico, Universidade de São Paulo, São Paulo 05508-120, Brazil

[4] Istituto di Geoscienze e Georisorse CNR, 56124 Pisa, Italy

[5] Dipartimento di Scienze Pure e Applicate (DiSPeA), Università degli Studi di Urbino "Carlo Bo", 61029 Urbino, Italy

[6] Present Address: Instituto de Geociências, Universidade de Brasília, Brasília 70910-900, Brazil

[7] Present Address: Instituto de Geociências, Universidade de São Paulo, São Paulo 05508-080, Brazil

[8] Department of Geological Engineering, Fırat University, Elazığ, Turkey

[9] EECB and Biology Department, University of Nevada, Reno, 1664 N. Virginia Street, Reno, NV 89557, USA